AFCRL-65-526

THE TRANSFER FUNCTION FOR P-WAVES FOR A SYSTEM CONSISTING OF A POINT SOURCE IN A LAYERED MEDIUM

KARL FUCHS
Saint Louis University
St. Louis, Missouri

Contract AF 19(604)-7399
Project No 8652
Task No. 865201

SCIENTIFIC REPORT NO. 12

July 1965

Prepared
for

Air Force Cambridge Research Laboratories
Office of Aerospace Research
United States Air Force
Bedford, Massachusetts

WORK SPONSORED BY ADVANCED RESEARCH PROJECTS AGENCY
PROJECT VELA UNIFORM

ARPA Order No. 292
Project Code No. 8100, Task 2

AFCRL-65-526

THE TRANSFER FUNCTION FOR P-WAVES FOR A SYSTEM CONSISTING OF A POINT SOURCE IN A LAYERED MEDIUM

KARL FUCHS

Saint Louis University

St. Louis, Missouri

Contract AF 19(604)-7399

Project No. 8652

Task No. 865201

SCIENTIFIC REPORT NO. 12

July 1965

Prepared

for

AIR FORCE CAMBRIDGE RESEARCH LABORATORIES

OFFICE OF AEROSPACE RESEARCH

UNITED STATES AIR FORCE

BEDFORD, MASSACHUSETTS

WORK SPONSORED BY ADVANCED RESEARCH PROJECTS AGENCY

PROJECT VELA-UNIFORM

ARPA Order No. 292

Project Code No. 8100, Task 2

Requests for additional copies by agencies of the Department of Defense, their contractors, or other government agencies should be directed to:

Defense Documentation Center (DDC)
Cameron Station
Alexandria, Virginia 22314

Department of Defense contractors must be established for DDC services or have their "need-to-know" certified by the cognizant military agency of their project or contract.

All other persons and organizations should apply to the:

Clearinghouse for Federal Scientific
and Technical Information (CFSTI)
Sills Building
5285 Port Royal Road
Springfield, Virginia 22151

ABSTRACT

This paper investigates in what manner the spectrum of body waves radiating from point sources in a multilayered medium over a homogeneous half-space is different from the spectrum of body waves from the same source in an infinite medium. The effect of the system consisting of a point source in a layered crust on the spectrum of p-waves observed at large distances in the half space is studied. Analytical expressions for the transfer function of this system are derived for three types of point sources: an explosive source, a single couple, and a double couple of arbitrary orientation within the crust.

Preliminary numerical computations for the explosive source at various depths in a realistic model of the earth's crust study the effect of: a) the angle of incidence into the homogeneous half-space, b) the source depth, c) minor variations of the crustal model. In the case of an explosive source the most influential parameter of the transfer function is the source depth. In shallow explosions the low frequency part of the spectrum of body waves is comparatively rejected.

Table of Contents

The Transfer Function for P-Waves for a System Consisting of a Point Source in a Layered Medium

Page

Figure Captions

Figure 1: Point Sources and the crust of th earth. An explosive source, a single, or a double couple radiate body waves into the mantle with angle of incidence γ p.

Figure 2: Cartesian (x,y,z) and cylindrical polar (r, Θ, z) coordinate system with numbering of layers, depth of interfaces and of source.

Figure 3: Contour integration in the complex k-plane.

Figure 4: Geometry of the single couple. The point forces $+\xi\vec{R}$ and $-\xi\vec{R}$ act on the line element $\xi\vec{R}$.

Figure 5: The influence of the angle of incidence on the amplitude of the transfer function of the system consisting of an explosive point source in the crustal model NOCR (right part of figure) - at depth 30 km. $\gamma = 75^\circ, 60^\circ, 45^\circ, 30^\circ, 15^\circ$ from top to bottom. Corresponding phase velocities are indicated.

Figure 6: Amplitude of the transfer function for the explosive source at depths 0.5, 8.0, 30.0 km in the crustal model NOCR. Angle of incidence $\gamma = 45^\circ$. Frequency range 0 - 0.3 cps.

Figure 7: Amplitude $|T|$ and phase δ of the transfer function for the explosive source at depth 0.5 km in the crustal model NOCR. Angle of incidence $\gamma = 45^\circ$. Frequence range 0 - 4.0 cps.

Figure 8: Amplitude $|T|$ and phase δ of the transfer function for the explosive source at depth 8.0 km in the crustal model NOCR. (See Figure 7)

Figure 9: Comparison of amplitude of the transfer functions for explosive source at depth 8 km, $\gamma = 30^\circ$ in crustal model NOCR, and modified models LVC1, LVC2 (see tables 1-3).

The Transfer Function for P-Waves for a System Consisting of a Point Source in a Layered Medium

1. Introduction.

Focal mechanism studies using body and surface wave observations endeavor to extract useful information about the source of an earthquake from the set of signals observed at seismic stations distributed over the world. Not all the information about the source originally contained in the signal in the neighborhood of the source will reach the stations at large distances from the source. There is, of course, loss of information due to geometrical spreading and to absorption. But equally as important, each homogeneity encountered by the signal along its path from the source to the receiver will more or less reshape the signal. A very strong deformation of the seismic signal occurs on its passage through the crust of the earth, since the dimensions of the crust are of the order of the dominant wave length of the signal.

For the case of deep focus earthquakes (source depth > 300 km) only the crust at the receiver has to be accounted for. But as soon as the source approaches the crust, interference between direct waves and reflected waves becomes a factor. In this circumstance the structure of the earth's crust at the source will also strongly deform the signal originally radiated from the point source. Espcecially is this the case if the source is located within the

crust. It is the purpose of this study to investigate how the spectrum of body waves radiating from a point source is affected if this point source is placed within the crust instead of in an infinite homogeneous and isotropic medium. This paper concentrates on the spectrum of dilatational waves radiated from three commonly used point source models (explosive source, single couple, and double couple) into the mantle.

The dilatational displacement potential in the mantle of the earth at large distances from the source will be calculated. Numerical examples for the case of the explosive source in the crust will be presented. For the sake of clarity the assumptions made throughout this paper concerning the nature of the model consisting of a point source in the crust will be listed here.

1.1 <u>Assumptions on the model "point source in the crust."</u>

The situation is depicted in figure 1. The assumptions are:

1. We are dealing with a point source, i.e. the dimensions of the source region should be small compared to the distance to the next boundary. With this limitation in mind the point source may be placed at any point in a layered medium.
2. The crust of the earth is approximated by a system of (n-1) homogeneous, isotropic layers with plane parallel interfaces. The P-, the S-wave velocity, the density, and the layer thickness for the i^{th}

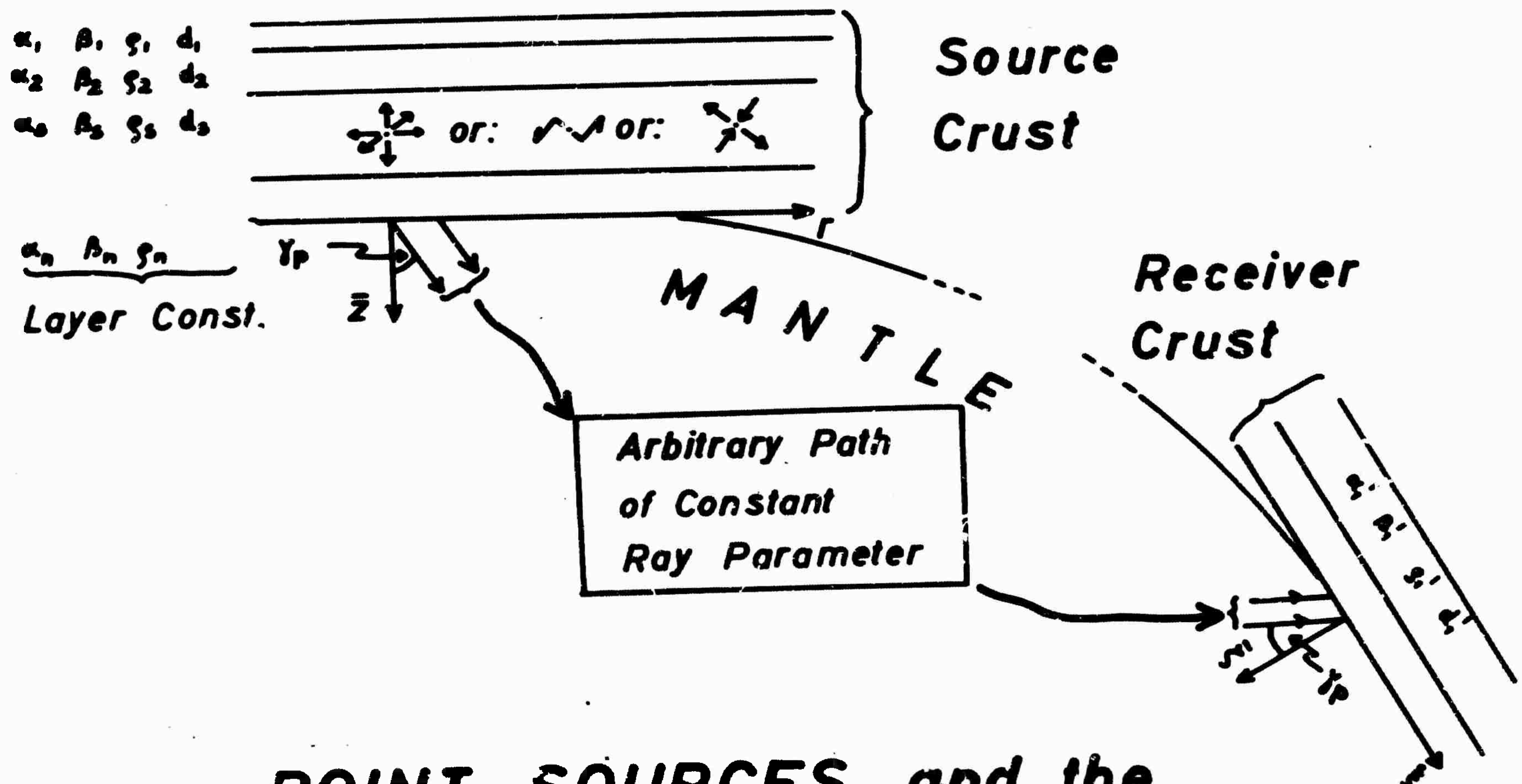

POINT SOURCES and the
CRUST of the EARTH

Figure 1

layer will be denoted by α_i, β_i, ρ_i and d_i respectively. The top layer is specified to have a free surface. The angle γ is the angle of incidence for P-waves in the mantle.

3. The mantle, the n^{th} layer, will be regarded to be "relatively homogeneous." By this we mean, quite generally speaking, that the elastic properties of the mantle vary much more gradually than they do in the crust. Thus we choose the n^{th} layer to be a homogeneous half-space.

From this point on, the word "crust" will mean the system of n-1 layers described under 1. The term "mantle" or "subcrustal material" refers to the homogeneous half-space of our model.

Figure 1 indicates furthermore, how the signal might be followed through the mantle to the base of the crust at the receiver station and through that crust to the receiver. In this paper we will not consider the influence of the mantle path or of the receiver crust on the signal. These latter effects have been examined by a number of authors. Ben-Menahem, et al. (1965) described a method for the recovery of source parameters if the source is located in a realistic mantle model sufficiently removed from the base to the crust. The influence of the receiver crust system has been treated recently by Phinney (1964), Hannon (1964a,b), Ben-Menahem, et al. (1965) using the matrix formulation of Thomson (1950) as developed by

Haskell (1953).

1.2 Previous investigations.

Elastic waves radiating from point sources in a multi-layered medium overlying a homogeneous half-space have been investigated recently by a number of authors. Harkrider (1964) formulated the solution for an explosive source, a vertical and a horizontal point force in a layered medium by the Thomson-Haskell matrix method in the frequency domain. He concentrated on the effect of the source crust on surface waves of Rayleigh and Love type.

Bortfeld (1964) reported on a solution in the time domain by a method of numerical interpretation.

Van Nostrand (1964) presented computations of synthetic seismograms at large distances from point sources in the crust. He also works completely in the time domain.

Dunkin (1965) applied integral transformation techniques for a refinement of the matrix formulation. His matrix formulation is especially useful for numerical calculations at high frequencies. He provides a review of the current Thomson-Haskell matrix method which gives a good insight into the purpose and significance of matrix methods in problems of wave propagation.

In this paper we shall now proceed in the following steps:

Section 2: The displacement potentials for P-waves due to a vertical and a horizontal point source in the crust will be derived as integral representation

(sections 2.1 and 2.2). A large distance approximation will be given in 2.3.

Section 3: The results for the vertical and horizontal point force are used to construct the potentials due to three types of point sources commonly used in focal mechanism studies: an explosive source, a single couple, and a double couple. Transfer functions for these systems "point source in the crust" will be defined there.

Section 4: Preliminary numerical examples for the case of the explosive source in the crust will be presented.

2.0 The displacement potential due to a vertical and a horizontal point force in a layered medium over half-space.

Throughout this paper we prefer to work in the frequency domain. The description of wave propagation by a frequency transfer function is, in many cases, more advantageous than the equivalent description by the system response to a unit pulse excitation, since in many studies the knowledge of the frequency response is required in any event, and since the overall transfer functions of a series of linear systems can more easily be obtained by multiplication of the corresponding transfer functions than by convolution of the corresponding unit pulse responses.

2.1 The displacement potential due to a vertical and a horizontal point force.

We shall consider the process of wave propagation

from a vertical and a horizontal point force in a layered medium over a half-space after transforming our model of the process in a timeless space by a Fourier integral transformation of the equations of motion for the various homogeneous layers of our model, including the source and boundary conditions. In such a space information from source to receiver is no longer transmitted in time. In this timeless space a local disturbance of the equilibrium at the source will "immediately" affect the whole system. Our transformed point source, a Dirac-delta-source in space, which acts either as a vertical or horizontal point force will generate a disturbance in the distribution of the stress-tensor. The stress-tensor is coupled to the strain tensor by the elasticity tensor. Therefore the redistribution of stresses will also cause a redistribution of the transformed displacement vector throughout the transformed space, right to the place of the receiver.

For the description of our model we choose the two coordinate systems depicted in figure 2. For the most part the cylindrical system (r, Θ, z) will be used. In Sect. 2.2 the right-handed xyz-system is sometimes more advantageous.

It will now be useful to define transformed displacement potentials $\bar{\varphi}_1$, $\bar{\psi}_1$ and $\bar{\chi}_1$ from which the transformed displacements vector ($\bar{q}_1$, $\bar{v}_1$, $\bar{w}_1$) may be derived (see Harkrider, 1964) as follows:

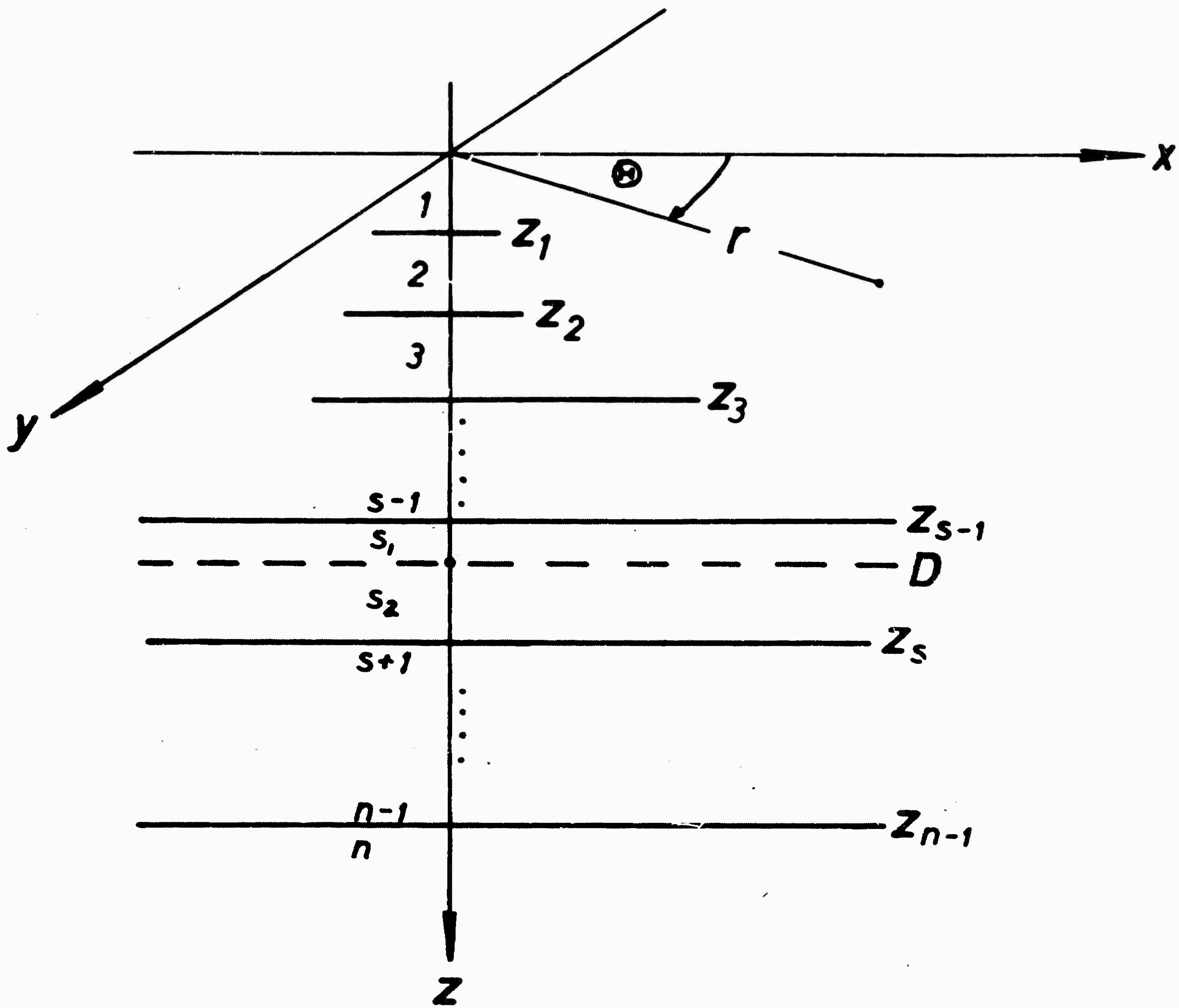

Figure 2

Figure 2

$$\bar{q}_i(r,\Theta,z) = \frac{\partial\bar{\varphi}_i}{\partial r} + \frac{\partial^2\bar{\psi}_i}{\partial r\,\partial z} + \frac{1}{r}\frac{\partial\bar{\chi}_i}{\partial\Theta} \tag{2.1}$$

$$\bar{v}_i(r,\Theta,z) = \frac{1}{r}\frac{\partial\bar{\varphi}_i}{\partial\Theta} + \frac{1}{r}\frac{\partial^2\bar{\psi}_i}{\partial z\,\partial\Theta} - \frac{\partial\bar{\chi}_i}{\partial r} \tag{2.2}$$

$$\bar{w}_i(r,\Theta,z) = \frac{\partial\bar{\varphi}_i}{\partial z} + \frac{\partial^2\bar{\psi}_i}{\partial z^2} + k_{\beta_i}^2\,\bar{\psi}_i \tag{2.3}$$

$$i = 1,\dots,n$$

We will then carry these potentials from the source to a "receiver" within the homogeneous half-space. Comparing these with the potentials which would have arisen if the same type of source had been placed in an infinite medium of subcrustal material, we arrive at the quotient of the two potentials which may be regarded as the transfer functions of the source crust system.

The potentials will not be carried directly from the source to receiver. The Thomson-Haskell matrix formulation uses the so-called motion-stress vector, whose components are the components of the displacement or particle velocity vector and of the stress tensor. This motion-stress vector is carried across the interface continuously, and through the layer from top to bottom by a matrix transformation. Thus the continuation of the motion-stress vector from source to receiver can be expressed as a series of matrix transformations. Dunkin (1965) reformulated the Thomson-Haskell

matrix method to reduce numerical difficulties at higher frequencies. Dunkin's refined matrix formulation allows, so to speak, an increased flow of information from source, to receiver through the "noisy channel" of a digital computer.

This paper will follow the matrix formulation as explicitly developed by Harkrider (1964). To avoid repetition we will simply sum up that he continues two motion-stress vectors $\vec{M}_{Ri}$ and $\vec{M}_{Li}$ through the model from source to receiver. In the ith layer these vectors are:

$$\vec{M}_{Ri} = \left\{ \frac{\dot{u}_{Ri}(z_i)}{c}, \frac{\dot{w}_{Ri}(z_i)}{c}, \sigma_{Ri}(z_i), \tau_{Ri}(z_i) \right\} \tag{2.4}$$

$$\vec{M}_{Li} = \left\{ \frac{\dot{v}_{Li}(z_i)}{c}, \tau_{Li}(z_i) \right\} \tag{2.5}$$

These vectors, which are dependent on only, are essentially derived by a series of integral transformations from the Fourier transformed displacement potentials. They are connected with the transformed potentials $\varphi_i(z), \psi_i(z), \chi_i(z)$

$$\frac{\dot{u}_{Ri}(z)}{c} = k^2 \left[\varphi_i(z) + \frac{d\,\psi_i(z)}{dz} \right] \tag{2.6}$$

$$\frac{\dot{w}_{Ri}(z)}{c} = i k \left[\frac{d\,\varphi_i(z)}{dz} + \frac{d^2\psi_i(z)}{dz^2} + k_{\beta i}\,\psi_i(z) \right] \tag{2.7}$$

$$\sigma_{Ri}(z) = 2\mu_i \left[\frac{d^2\varphi_i(z)}{dz^2} + \frac{d^3\psi_i(z)}{dz^3} + k^2_{\beta_i} \frac{d\psi_i(z)}{dz} \right] - \lambda_i k^2_{\alpha_i} \varphi_i(z) \qquad (2.8)$$

$$\tau_{Ri}(z) = -i k \mu_i \left[2 \frac{d\varphi_i(z)}{dz} + 2 \frac{d^2\psi_i(z)}{dz^2} + k^2_{\beta_i} \psi_i(z) \right] \qquad (2.9)$$

and

$$\frac{\dot{v}_{Li}(z)}{c} = i k^2 \chi_i(z) \qquad (2.10)$$

$$\tau_{Li}(z) = k \mu_i \frac{d\chi_i(z)}{dz} \qquad (2.11)$$

In eq. (2.6) - (2.11) the following notations are used:

$k = \frac{\omega}{c}$: horizontal wave number, with
c = horizontal phase velocity

k_{α_i} dilatational } wave number with α_i = p-velocity in } i^{th} layer
k_{β_i} shear } β_i = S-velocity in }

Lame's constants in the i^{th} layer

From $\varphi_i(z)$, $\psi_i(z)$, $\chi_i(z)$ the Fourier transformed displacement potentials $\bar{\varphi}_i$, $\bar{\psi}_i$, $\bar{\chi}_i$ are obtained by:

$$\bar{\varphi}_i(r, \Theta, z) = \int_0^\infty \varphi_i(z)\, J_\ell(kr) \cos \ell\Theta \, dk \qquad (2.12)$$

$$\bar{\psi}_i(r, \Theta, z) = \int_0^\infty \psi_i(z)\, J_\ell(kr) \cos \ell\Theta \, dk \qquad (2.13)$$

$$\bar{\chi}_i(r, \Theta, z) = \int_0^\infty \chi_i(z)\, J_\ell(kr) \sin \ell\Theta \, dk \qquad (2.14)$$

J_ℓ are the Bessel functions of order ℓ, where $\ell = 0, 1$ in case of vertical and horizontal point force respectively.

This paper will only be concerned with the P-waves radiating into the half-space. Therefore we will now only follow the motion-stress vector $\vec{M}_{Ri}$ from source to receiver. This vector is continued from top of layer i to the bottom of the layer i by the matrix relation:

$$\vec{M}_{Ri}(z_i) = a_{R_i} \cdot \vec{M}_{Ri}(z_{i-1}) \qquad i = 1, \dots, n \tag{2.15}$$

The elements of the matrix a_{R_i}, the layer matrix, are:

$$
\begin{aligned}
(a_{R_i})_{11} &= (a_{R_i})_{44} = \gamma_i \cos P_i - (\gamma_i - 1)\cos Q_i \\
(a_{R_i})_{12} &= (a_{R_i})_{34} = i\left[(\gamma_i - 1)\frac{\sin P_i}{r_{\alpha_i}} + \gamma_i r_{\beta_i} \sin Q_i\right] \\
(a_{R_i})_{13} &= (a_{R_i})_{24} = -(\rho_i c^2)^{-1}\left[\cos P_i - \cos Q_i\right] \\
(a_{R_i})_{14} &= i(\rho_i c^2)^{-1}\left[\frac{\sin P_i}{r_{\alpha_i}} + r_{\beta_i} \sin Q_i\right] \\
(a_{R_i})_{21} &= (a_{R_i})_{43} = -i\left[\gamma_i r_{\alpha_i} \sin P_i + (\gamma_i - 1)\frac{\sin Q_i}{r_{\beta_i}}\right] \\
(a_{R_i})_{22} &= (a_{R_i})_{33} = -(\gamma_i - 1)\cos P_i + \gamma_i \cos Q_i \\
(a_{R_i})_{23} &= i(\rho_i c^2)^{-1}\left[r_{\alpha_i} \sin P_i + \frac{\sin Q_i}{r_{\beta_i}}\right] \\
(a_{R_i})_{31} &= (a_{R_i})_{42} = \rho_i c^2 \gamma_i (\gamma_i - 1)\left[\cos P_i - \cos Q_i\right] \\
(a_{R_i})_{32} &= i \rho_i c^2\left[(\gamma_i - 1)^2 \frac{\sin P_i}{r_{\alpha_i}} + \gamma_i^2 r_{\beta_i} \sin Q_i\right] \\
(a_{R_i})_{41} &= i \rho_i c^2\left[\gamma_i^2 r_{\alpha_i} \sin P_i + (\gamma_i - 1)^2 \frac{\sin Q_i}{r_{\beta_i}}\right]
\end{aligned}
\tag{2.16}
$$

where:

$$\gamma_i = 2\left(\frac{\beta_i}{c}\right)^2 \tag{2.17}$$

$$P_i = k\, r_{\alpha_i}\, d_i \tag{2.18}$$

$$Q_i = k\, r_{\beta_i}\, d_i \tag{2.19}$$

$$d_i = z_i - z_{i-1} \tag{2.20}$$

and:

$$k r_{\alpha_i} = \begin{cases} -i\sqrt{k^2 - k_{\alpha_i}^2} & \text{for } k > k_{\alpha_i} \\ \sqrt{k_{\alpha_i}^2 - k^2} & \text{for } k < k_{\alpha_i} \end{cases} \tag{2.21}$$

$$k r_{\beta_i} = \begin{cases} -i\sqrt{k^2 - k_{\beta_i}^2} & \text{for } k > k_{\beta_i} \\ \sqrt{k_{\beta_i}^2 - k^2} & \text{for } k < k_{\beta_i} \end{cases} \tag{2.22}$$

Since the motion-stress vector is continuous across the interfaces it can be continued directly into the next layers until the receiver point is reached. Harkrider then shows that the point forces can be represented in our z-dependent model space by introducing a discontinuity of the motion-stress vector at the place $z = D$ of the source. These discontinuous motion-stress vectors are in case of a vertical point source:

$$\{0,\ 0,\ \delta\sigma_{R_s},\ 0\} \tag{2.23}$$

where

$$\delta\sigma_{R_s} = -\frac{\bar{L}\, k}{2\pi} \tag{2.24}$$

and for a horizontal point force:

$$\{ 0, \ 0, \ 0, \ \delta\tau_{R_s} \} \tag{2.25}$$

where

$$\delta\tau_{R_s} = i \frac{\bar{L}k}{2\pi} \tag{2.26}$$

$\bar{L}(\omega)$ is the Fourier transformed point force. Now the source layer $i = s$ is divided into two layers s_1 and s_2 at the level of the source depth D (see figure 2). The layer s_1 will be referred to as the top source layer. The layer matrix $a_{R_{s1}}$ for the layer s_1 are the same as for the undivided source layer s only $d_s = z_s - z_{s-1}$ has to be replaced by ζ, the depth of the source in the source layer.

Taking care of the prescribed components of the motion-stress vector at the free surfaces and the radiation condition that no sources are at infinity, one is in a position to continue the motion-stress vector introduced at the source to the receiver position in the infinite half-space. In the half-space n the transformed potential in the form:

$$\varphi_n(z) = -\left(\frac{\alpha_n}{\omega}\right)^2 e^{-ikr_{\alpha_n}(z-z_{n-1})} \Delta_j \tag{2.27}$$

$$\psi_n(z) = -i\frac{\gamma_n}{k^2} e^{-ikr_{\beta_n}(z-z_{n-1})} \omega_j \tag{2.28}$$

$$j = V \text{ or } H$$

satisfies the wave equations and the radiation conditions, provided kr_{α_n} and kr_{β_n} are chosen as in eq. (2.21), (2.22). In that case Δ_j and ω_j are connected with the motion-stress vector $\vec{M}_{R_n}$ in the half-space by the matrix relation:

$$\begin{bmatrix} \Delta_j \\ \Delta_j \\ \omega_j \\ \omega_j \end{bmatrix} = E^{-1}_{R_n} \cdot \vec{M}_{R_n} \qquad j = V \text{ or } H \tag{2.29}$$

where:

$$E^{-1}_{R_i} = \begin{bmatrix} -2\left(\frac{\beta_i}{\alpha_i}\right) & 0 & (\rho_i \alpha_i^2)^{-1} & 0 \\ 0 & c^2(\gamma_i - 1)/(\alpha_i^2 r_{\alpha_i}) & 0 & (\rho_i \alpha_i^2 r_{\alpha_i})^{-1} \\ (\gamma_i - 1)/(\gamma_i r_{\beta_i}) & 0 & -(\rho_i c^2 \gamma_i r_{\beta_i})^{-1} & 0 \\ 0 & 1 & 0 & (\rho_i c^2 \gamma_i)^{-1} \end{bmatrix} \tag{2.30}$$

The following matrix relations connect the potential vector defined in eq. (2.28) with the motion-stress vector $\vec{M}_{R_1}(0)$ at the free surface and the source motion-stress vector:

a) for a vertical point force:

$$\begin{bmatrix} \Delta_V \\ \Delta_V \\ \omega_V \\ \omega_V \end{bmatrix} = J \cdot \begin{bmatrix} \frac{\dot{u}_{R_1}(0)}{c} \\ \frac{\dot{w}_{R_1}(0)}{c} \\ 0 \\ 0 \end{bmatrix} + A^{-1}_{R_{s1}} \cdot \begin{bmatrix} 0 \\ 0 \\ \delta\sigma_{R_s} \\ 0 \end{bmatrix} \tag{2.31}$$

b) for a horizontal point force in direction $\Theta = 0^\circ$ (see figure 2):

$$\begin{bmatrix} \Delta_H \\ \Delta_H \\ \omega_H \\ \omega_H \end{bmatrix} = J \cdot \begin{bmatrix} \frac{\dot{u}_{R_1}(0)}{c} \\ \frac{\dot{w}_{R_1}(0)}{c} \\ 0 \\ 0 \end{bmatrix} + A^{-1}_{R_{s1}} \cdot \begin{bmatrix} 0 \\ 0 \\ 0 \\ \delta\tau_{R_s} \end{bmatrix} \tag{2.32}$$

where

$$J = E^{-1}_{R_n} \cdot a_{R_{n-1}} \cdot \ldots \cdot a_{R_1} \tag{2.33}$$

will be called the crustal matrix and where $A_{R_{s1}}^{-1}$ is the
verse of

$$A_{R_{s1}} = a_{R_{s1}} \cdot a_{R_{s-1}} \cdot \ldots \cdot a_{R_1} \tag{2.34}$$

A_{R_s} will be termed the top source matrix, while $a_{R_{s1}}$ is the top layer matrix. Harkrider (1964) derives a very convenient form for the elements of $A_{R_{s1}}^{-1}$:

$$A_{R_{s1}}^{-1} = \begin{bmatrix} (A_{R_{s1}})_{44} & -(A_{R_{s1}})_{34} & (A_{R_{s1}})_{24} & -(A_{R_{s1}})_{14} \\ -(A_{R_{s1}})_{43} & (A_{R_{s1}})_{33} & -(A_{R_{s1}})_{23} & (A_{R_{s1}})_{13} \\ (A_{R_{s1}})_{42} & -(A_{R_{s1}})_{32} & (A_{R_{s1}})_{22} & -(A_{R_{s1}})_{12} \\ -(A_{R_{s1}})_{41} & (A_{R_{s1}})_{31} & -(A_{R_{s1}})_{21} & (A_{R_{s1}})_{11} \end{bmatrix} \tag{2.35}$$

In case of the vertical point source we are only concerned with the matrix eq. (2.31), for the horizontal point force with eq. (2.32). Both matrix equations represent each a system of 4 linear algebraic equations for the 4 unknowns $\Delta_V, \omega_V, \dot{u}_{R_1}(0)/c, \dot{w}_{R_1}(0)/c$ or $\Delta_H, \omega_H, \dot{u}_{R_1}(0)/c, \dot{w}_{R_1}(0)/c$ respectively.

Up to this point we have followed Harkrider's development. Since he was interested in the surface displacements, he solved the systems of equations for $\frac{\dot{u}_{R_1}(0)}{c}$, $\frac{\dot{w}_{R_1}(0)}{c}$ arriving finally at the displacements due to surface waves of the Rayleigh type.

Since in this paper we are interested in the radiation of P waves into the half-space we shall solve the systems for Δ_V and Δ_H, corresponding to P waves from the vertical and horizontal point force. Given these quantities we then

derive integral representations for the transformed potentials $\bar{\varphi}_{nV}$ due to a vertical point source:

$$\bar{\varphi}_{nV}(r,z) = \int_0^\infty (-1)\, \Delta_V \left(\frac{\alpha_n}{\omega}\right)^2 e^{-ikr_{\alpha_n}(z-z_{n-1})} J_0(kr)\, dk \qquad (2.36)$$

and $\bar{\varphi}_{nH}$ due to a horizontal point force:

$$\bar{\varphi}_{nH}(r,\theta,z) = \int_0^\infty \cos\theta\, (-1)\, \Delta_H \left(\frac{\alpha_n}{\omega}\right)^2 e^{-ikr_{\alpha_n}(z-z_{n-1})} J_1(kr)\, dk \qquad (2.37)$$

Solving (2.31) for Δ_V results in:

$$\Delta_V = \frac{D_1}{D_R} \qquad (2.38)$$

where:

$$D_1 = U\left[(J_{31}-J_{41})(J_{13}J_{22}-J_{12}J_{23})+(J_{42}-J_{32})(J_{21}J_{13}-J_{11}J_{23})+(J_{33}-J_{43})(J_{21}J_{12}-J_{11}J_{22})\right]+$$
$$V\left[(J_{31}-J_{41})(J_{22}J_{14}-J_{12}J_{24})+(J_{42}-J_{32})(J_{14}J_{21}-J_{11}J_{24})+(J_{34}-J_{44})(J_{21}J_{12}-J_{11}J_{22})\right] \qquad (2.39)$$

$$D_R = (J_{11}-J_{21})(J_{32}-J_{42}) - (J_{12}-J_{22})(J_{31}-J_{41}) \qquad (2.40)$$

J_{km} are the elements of the crustal matrix J (eq. (2.33)), and U and V (using eq. (2.35)) are given by:

$$U = (A_{R_{S1}})^{-1}_{33}\, \delta\sigma_{R_S} + (A_{R_{S1}})^{-1}_{34}\, \delta\tau_{R_S} = (A_{R_{S1}})_{22}\, \delta\sigma_{R_S} - (A_{R_{S1}})_{12}\, \delta\tau_{R_S} \qquad (2.41)$$

$$V = (A_{R_{S1}})^{-1}_{43}\, \delta\sigma_{R_S} + (A_{R_{S1}})^{-1}_{44}\, \delta\tau_{R_S} = -(A_{R_{S1}})_{21}\, \delta\sigma_{R_S} + (A_{R_{S1}})_{11}\, \delta\tau_{R_S} \qquad (2.42)$$

In case of a vertical point source (see eq. (2.23),(2.24)) we have

$$U_V = -\frac{Lk}{2\pi}(A_{R_{S1}})_{22}$$
$$V_V = +\frac{Lk}{2\pi}(A_{R_{S1}})_{21} \qquad (2.43)$$

and for the horizontal point force eq. (2.41) and (2.42) degenerate to (see eq. (2.25), (2.26)):

$$U_H = -i \frac{\bar{L} k}{2\pi} \left(A_{R_{S1}} \right)_{12} \tag{2.44}$$

$$V_H = +i \frac{\bar{L} k}{2\pi} \left(A_{R_{S1}} \right)_{11} \tag{2.45}$$

Considering that $\frac{\bar{L} k}{2\pi}$ is a common factor in the quantities U and V and therefore a factor of Δ_V and Δ_H we shall define for later use the quantities $\bar{\Delta}_V$ and $\bar{\Delta}_H$ by:

$$\Delta_V = - \frac{\bar{L} k}{2\pi} \bar{\Delta}_V \tag{2.46}$$

$$\Delta_H = - \frac{\bar{L} k}{2\pi} \bar{\Delta}_H \tag{2.47}$$

The eq. (2.36) and (2.37) represent the complete solutions for the dilatational displacement potential within the half-space due to a vertical or a horizontal point force in a layered crust. In the next section 2.2 we will use contour integration in the complex k-plane to separate modal solutions of the surface wave type from the contributions of body waves.

2.2 Separation of modal surface wave solutions from body waves

The procedure for the separation of modal surface wave contributions from body waves will be described only for the transformed dilatational potential $\bar{\varphi}_{nV}$ due to a vertical point source. The separation in case of the horizontal point force follows the same line of reasoning.

The dilatational potential $\bar{\varphi}_{nV}(r,z)$ in the half-space

due to a vertical point source is given by eq. (2.36), which we rewrite using eq. (2.46):

$$\bar{\varphi}_{nv}(r,z) = \int_0^{\infty} \frac{\bar{L}k}{2\pi} \left(\frac{\alpha_n}{\omega}\right)^2 \bar{\Delta}_v(k)\, e^{-ikr_{\alpha_n}\bar{z}} J_0(kr)\, dk \tag{2.48}$$

where: $$\bar{z} = z - z_{n-1} \tag{2.49}$$

and kr_{α_n} is the same as defined in eq. (2.21). To evaluate the integral in (2.48) we use contour integration in the complex -plane. We will introduce the following abbreviation:

$$F(k) = \frac{\bar{L}k}{2\pi} \left(\frac{\alpha_n}{\omega}\right)^2 \bar{\Delta}_v(k) \tag{2.50}$$

The Bessel function will be replaced by the Hankel functions:

$$J_0(kr) = \frac{1}{2}\left[H_0^{(1)}(kr) + H_0^{(2)}(kr)\right] \tag{2.51}$$

With this equation (2.48) may be written as:

$$\bar{\varphi}_{nv}(r,z) = I_1 + I_2 \tag{2.52}$$

where:

$$I_1 = \frac{1}{2}\int_0^{\infty} F(k)\, e^{-ikr_{\alpha_n}\bar{z}} H_0^{(1)}(kr)\, dk \tag{2.53}$$

$$I_2 = \frac{1}{2}\int_0^{\infty} F(k)\, e^{-ikr_{\alpha_n}\bar{z}} H_0^{(2)}(kr)\, dk \tag{2.54}$$

From now on we consider the wave number k and the angular frequency ω to be complex variables:

$$\zeta = k + i\tau \tag{2.55}$$

$$\omega = s - it \tag{2.56}$$

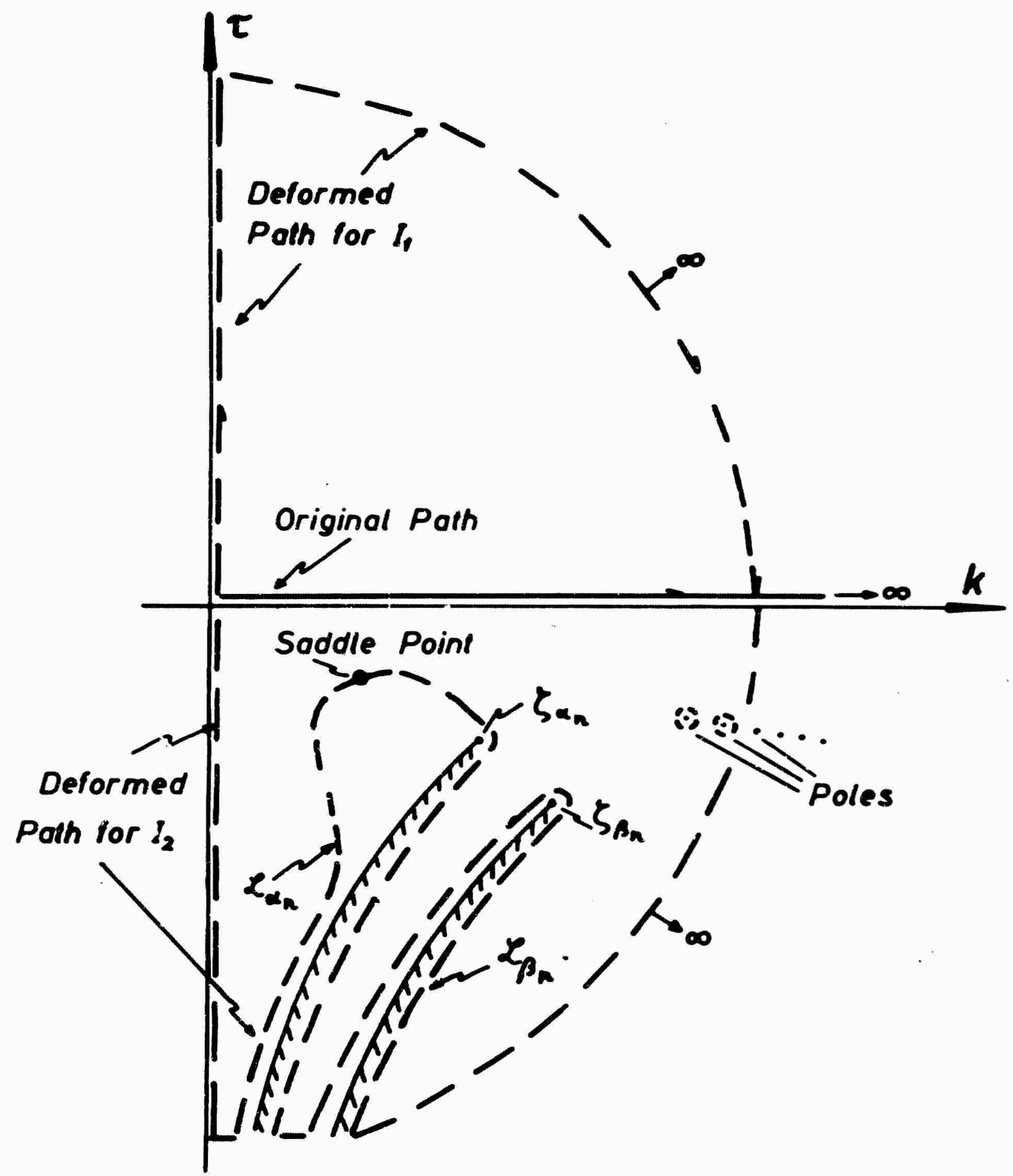
τ
Deformed
Path for I_1
∞
Original Path
∞
k
Saddle Point
ζ_{α_n}
Poles
ζ_{β_n}
Deformed
Path for I_2
$\mathcal{L}_{\alpha_n}$
∞
$\mathcal{L}_{\beta_n}$

Figure 5

Figure 3

Keeping in mind that

$$\lim_{\zeta r \to +\infty} H_0^{(1)}(\zeta r) = 0 \quad \text{for} \quad k>0,\ \tau>0 \qquad (2.57)$$

$$\lim_{\zeta r \to -\infty} H_0^{(2)}(\zeta r) = 0 \quad \text{for} \quad k>0,\ \tau<0 \qquad (2.58)$$

we displace the path of integration from the positive real axis to the imaginary axis for the integral I_1, containing $H_0^{(1)}$, and to the negative imaginary axis for the integral I_2 containing $H_0^{(2)}$, closing the path by the quarter circle in the first and fourth quadrant, respectively. The contribution to the integrals I_1 and I_2 along these quarter circles vanish according to eq. (2.57) and (2.58).

The chosen deformation of the original contour is indicated in figure 3. The integrands in I_1 and I_2 have poles and are multivalued functions of ζ. The poles occur at the zeros of the denominator of $F(k)$. There is a singularity at $\zeta=0$ for the Hankel functions. This singularity disappears as both integrals are summed up, since the Bessel function is regular at $\zeta=0$. It will therefore be disregarded.

Due to the presence of the expressions $kr_{\alpha i}, kr_{\beta i}\ (i=1,\dots,n)$ which appear in the crustal matrix J, the integrand is multivalued. To get a single valued function we must introduce $2n$ branchlines originating at the branch points $\zeta r_{\alpha i}, \zeta r_{\beta i}\ (i=1,\dots,n)$. To assume the vanishing of the potential for $\zeta \to \infty$ we must remain on that sheet of

the Riemann surface where

$$\mathrm{Re}(i\zeta r_{\alpha_i}) > 0 \; ; \; \mathrm{Re}(i\zeta r_{\beta_i}) > 0 \qquad i = 1, \ldots, n \tag{2.59}$$

Therefore the branch lines are given by:

$$\mathrm{Re}(i\zeta r_{\alpha_i}) = 0 \tag{2.60}$$

$$\mathrm{Re}(i\zeta r_{\beta_i}) = 0 \qquad i = 1, \ldots, n \tag{2.61}$$

The positions of the poles and branchlines are indicated in figure 3 for the case of $\mathrm{Re}(\omega) > 0$. For $\mathrm{Re}(\omega) < 0$ the poles and branchlines would be displaced to the first quadrant. But the results of the following derivations are the same in both cases.

Jardetzky (1953) pointed out that in all cases of wave propagation from a point source in a multilayered medium over the half-space, all expected branch line integrals vanish except one branchline in each potential $\bar{\varphi}$ and $\bar{\Psi}$ corresponding to the terms r_{α_n} or r_{β_n}, respectively, for the half-space. (See also Ewing et al. (1957)). This can also be proven by considering the symmetry properties of the layer matrices a_{R_i} (see eq. (2.16)) and $E_{R_n}^{-1}$ (see eq. (2.30)). In this way it is possible to prove the vanishing of the branchline integrals due to $r_{\alpha_i}, r_{\beta_i}$ for $i = 1, \ldots, n-1$. There still remain two branchline contributions $\mathcal{L}_{\alpha_n}$ and $\mathcal{L}_{\beta_n}$ due to r_{α_n} and r_{β_n} of the half-space for both dilatational and shear potential.

Referring to figure 3 the contributions to the integrals I_1 and I_2 from branchlines and poles may be written as follows:

$$I_1 = \frac{i}{2}\int_0^{\infty} F(i\tau)\, e^{-i\zeta r_{\alpha n}\bar{z}}\, H_0^{(1)}(i\tau r)\, d\tau \tag{2.62}$$

$$I_2 = \frac{i}{2}\int_0^{-\infty} F(i\tau)\, e^{-i\zeta r_{\alpha n}\bar{z}}\, H_0^{(2)}(i\tau r)\, d\tau + \tag{2.63}$$

$$+\frac{1}{2}\int_{\mathcal{L}_{\alpha n}} \cdots \qquad +\frac{1}{2}\int_{\mathcal{L}_{\beta n}} \cdots \quad - 2\pi i \sum \text{Residues}$$

It can be shown that

$$F(i\tau) = -F(-i\tau) \tag{2.64}$$

Considering further that

$$H_0^{(1)}(i\tau r) = -H_0^{(2)}(-i\tau r) \tag{2.65}$$

we may write I_1 as:

$$I_1 = -\frac{i}{2}\int_0^{-\infty} F(i\tau)\, e^{-i\zeta r_{\alpha n}\bar{z}}\, H_0^{(2)}(i\tau r)\, d\tau \tag{2.66}$$

Summing I_1 and I_2 according to eq. (2.52) we realize that the contributions along the positive and the negative imaginary axes cancel. Therefore the final complete solution for $\bar{\varphi}_{nv}(r,z)$ is:

$$\bar{\varphi}_{nv}(r,z) = \frac{1}{2}\int_{\mathcal{L}_{\alpha n}} F(\zeta)\, e^{-i\zeta r_{\alpha n}\bar{z}}\, H_0^{(2)}(\zeta r)\, d\zeta + \tag{2.67}$$

$$+\frac{1}{2}\int_{\mathcal{L}_{\beta n}} F(\zeta)\, e^{-i\zeta r_{\beta n}\bar{z}}\, H_0^{(2)}(\zeta r)\, d\zeta - 2\pi i \sum \text{Residues}$$

Up to eq. (2.67) no approximation has been used. Thus eq.(2.67)

represents the exact solution for the Fourier transformed dilatational potential $\bar{\varphi}_{nv}(r,z)$ in the half-space due to a vertical point source within the crust.

We can now separate body waves from surface wave contributions by the following line of reasoning. Body waves may be regarded as those waves which travel in the half-space with horizontal phase velocity $c > \beta_n$. All waves traveling with phase velocity $c \leq \beta_n$ are more or less trapped in the crust, i.e. the amplitude diminishes rapidly within the half-space with increasing depth z. They are mathematically described by the residue contributions from the poles. Thus we may regard the contributions from the branchline contours as describing the body waves in the half-space generated by the point source in the layered medium.

We now define the transformed dilatational potential of body waves $\bar{\varphi}_v$ in the halfspace due to a vertical point source by:

$$\bar{\varphi}_v(r,z) = \frac{1}{2}\int_{\chi_{\alpha_n}} F(\zeta)\, e^{-i\zeta r_{\alpha_n}\bar{z}}\, H_0^{(2)}(\zeta r)\, d\zeta + \frac{1}{2}\int_{\chi_{\beta_n}} F(\zeta)\, e^{-i\zeta r_{\alpha_n}\bar{z}}\, H_0^{(2)}(\zeta r)\, d\zeta \qquad (2.68)$$

This definition of body waves is especially useful at large distances from the source such that the surface waves have had sufficient time to separate from the body waves. We shall now restrict our attention to the value of the integral representation of $\bar{\varphi}_v(r,z)$ at large distances from the source.

2.3 Large distance approximation.

At large distances from the source we substitute the approximation of the Hankel functions for large values of the argument ζr into eq. (2.[illegible]), writing the two integrals in one as:

$$\bar{\varphi}_v(r,z) = \int_{\mathcal{L}_{\alpha_n},\mathcal{L}_{\beta_n}} \frac{F(\zeta)}{\sqrt{2\pi\zeta r}} e^{-i(\zeta r_{\alpha_n}\bar{z} + \zeta r - \frac{\pi}{4})} d\zeta \tag{2.69}$$

For large distances we shall approximate the value of this integral by the contribution at the saddle point. To apply the saddle point method we rewrite the integral in the form:

$$\bar{\varphi}_v(r,z) = \int_{\mathcal{L}_{\alpha_n},\mathcal{L}_{\beta_n}} \frac{F(\zeta)}{\sqrt{2\pi\zeta r}} e^{f(\zeta)} d\zeta \tag{2.70}$$

where

$$f(\zeta) = -i(\zeta r_{\alpha_n}\bar{z} + \zeta r - \frac{\pi}{4}) \tag{2.71}$$

Since we are considering only the branchline integrals where there are no poles of $F(\zeta)$ on the chosen branch of the Riemann surface, we are justified in assuming that the factor of $\exp\{f(\zeta)\}$ varies slowly compared to $\exp\{f(\zeta)\}$ itself, especially for large r. In the fourth quadrant the saddle point of the integrand is determined from $f'(\zeta_0)=0$ to be located at:

$$\zeta_0 = \frac{r}{R}\zeta_{\alpha_n} \tag{2.72}$$

where

$$R = \sqrt{\bar{z}^2 + r^2} \tag{2.73}$$

is the distance from the plumb point of the source at the base of the crust to the receiver at $(r, \bar{z})$. Since always

$$r \leq R \tag{2.74}$$

one may conclude that, as long as R is sufficiently greater than r , i.e. as long as the receiver is sufficiently removed from the base of the crust, the saddle point is separated from the branch point at ζ_{α_n}.

Writing the complex branchpoint ζ_{α_n} as:

$$\zeta_{\alpha_n} = | \zeta_{\alpha_n} | \, e^{-i\varepsilon} \tag{2.75}$$

the path of steepest descent through the saddle point, on which $Re\{ f(\zeta)\}$ has a maximum and decreases most rapidly has the direction ϕ :

$$\phi = \frac{\pi}{4} - \frac{\varepsilon}{2} \tag{2.76}$$

Evaluation of (2.69) at the saddle point along the path of steepest descent yields finally

$$\bar{\varphi}_v (r, \bar{z}) = F(k_0) \, \frac{\bar{z}}{r R} \, e^{-i(k_{\alpha_n} R - \frac{\pi}{2})} \tag{2.77}$$

Here we have returned to real angular frequency ω and real wave number k . Since

$$\frac{r}{R} = \sin\gamma = \frac{\alpha_n}{c} \tag{2.78}$$

and since

$$k_{\alpha_n} = \frac{\omega}{\alpha_n} \tag{2.79}$$

the saddle point k_0 is located at:

$$k_0 = \frac{r}{R} \, k_{\alpha_n} = \frac{\alpha_n}{c} \; \frac{\omega}{\alpha_n} = \frac{\omega}{c} = k \tag{2.80}$$

Together with eq. (2.50) for $T(k)$ we may therefore write:

$$\bar{\varphi}_v(r,z) = i\,\frac{I\,k}{2\pi}\left(\frac{\alpha_n}{\omega}\right)^2 r_{\alpha_n}\,\bar{\Delta}_v\,\frac{e^{-i k_{\alpha_n} R}}{R} \qquad (2.81)$$

where use has been made of:

$$\frac{\bar{z}}{r} = \mathrm{ctg}\,\gamma = r_{\alpha_n} \qquad (2.82)$$

γ is the angle of incidence at which the P-waves leave the base of the crust (see figure 1).

The equivalent result for the dilatational potential due to a horizontal point force with direction $\Theta = 0^0$ is:

$$\bar{\varphi}_{H,0}(r,\Theta,z) = -\frac{I\,k}{2\pi}\left(\frac{\alpha_n}{\omega}\right)^2 r_{\alpha_n}\,\bar{\Delta}_H \cos\Theta\,\frac{e^{-i k_{\alpha_n} R}}{R} \qquad (2.83)$$

In the next section we shall now derive the expressions for three types of point forces commonly used as models in focal mechanism studies, namely: an explosive point source, a single couple and a double couple.

3.0 The transfer function for P-waves at large distances from three types of point sources: explosive source, single couple, and double couple.

3.1 Procedure and general remarks.

In this section we shall derive the transformed potentials at large distances for the following types of point sources:

1. Explosive point source, potential $\bar{\varphi}_1$ in 3.2
2. Single couple, potential $\bar{\varphi}_2$ in 3.3
3. Double couple, potential $\bar{\varphi}_3$ in 3.4.

These multipole types of point sources can be derived from a single point force by spatial differentiation and superposition (Ewing, et al. 1957). We shall take advantage of

the fact that the displacement field due to a point force of arbitrary orientation in a layered system can be composed by superposition of the fields due to the normal (vertical) and the tangential (horizontal) component of that point force (Keylis-Borok, 1953).

We wish to compare the potentials of the point source in the layered medium and of the point source in the infinite medium of subcrustal material. The latter potential we shall denote by $\bar{\varphi}_{i\infty}$, where $i = 1, 2, 3$ depending on the source type. We shall define functions:

$$T_i = \frac{\bar{\varphi}_i}{\bar{\varphi}_{i\infty}} \qquad i = 1, 2, 3$$

which we shall call transfer functions. They can be interpreted as describing the effect of the following operations on the particular type of point source in the infinite homogeneous medium of subcrustal material:

1) Replacing the half-space on top of the point source by a system of (n-1) different homogeneous layers with paralell interfaces.
2) Moving the point source into the s^{th} layer, the source layer.

Therefore we shall call for $i = 1, 2, 3$:

T_1 : dilatational transfer function of the system "type i point source in the crust" at large distances.

T_1 has been defined as the transfer function for the dilatational potential. It should be mentioned that any quantity derived from the dilatational potential, such as displacement,

particle velocity, etc., has the same transfer function as long as one is operating in the same way on the "input" $\bar{\varphi}_{i\infty}$ and the "output" $\bar{\varphi}_i$.

For all three types of point sources considered here the following explanations apply:

1) A point force may act in the arbitrary direction of the unit vector $\vec{n}$, which may be defined by its components in our xyz-coordinate system:

$$\vec{n} = \{ n_1, n_2, n_3 \} \tag{3.2}$$

We shall decompose the point force $\vec{K}$ into its component vectors:

$$\vec{K}_1 = \{ n_1 K, 0, 0 \} \tag{3.3}$$
$$\vec{K}_2 = \{ 0, n_2 K, 0 \} \tag{3.4}$$
$$\vec{K}_3 = \{ 0, 0, n_3 K \} \tag{3.5}$$

where $K = |\vec{K}|$

We are now dealing with one vertical, $\vec{K}_3$, and two horizontal point forces, $\vec{K}_1$ and $\vec{K}_2$. The potentials $\bar{\varphi}_{iV}$ and $\bar{\varphi}_{iH}$ due to these vertical and horizontal components are obtained from the expressions (2.81) and (2.83) derived in section 2.3 by taking into account the decomposition of the force. This means that in the motion-stress vector (eq. (2.23) and (2.25)) we have to replace $\bar{L}$ by $\bar{L} n_1$ or $\bar{L} n_2$ or $\bar{L} n_3$ for the three components of the point force.

2) The potentials $\bar{\varphi}'_V$ and $\bar{\varphi}'_H$ due to decomposed couples of forces (that is, a pair of equal but opposite

forces $\frac{K}{\varepsilon}\vec{n}$ acting at the ends of an infinitesimal line element $\varepsilon\vec{m}$, where $\vec{m}$ is the unit vector in the direction of the line), these potentials are obtained from $\bar{\varphi}_V$ and $\bar{\varphi}_H$ by taking the component of the gradient of these potentials in the direction of $\vec{m}$ (see for instance Nakano (1923)):

$$\bar{\varphi}'_V = \varepsilon\vec{m} \cdot \frac{1}{\varepsilon}\nabla_s\bar{\varphi}_V = \vec{m}\cdot\nabla_s\bar{\varphi}_V \tag{3.6}$$

$$\bar{\varphi}'_H = \varepsilon\vec{m} \cdot \frac{1}{\varepsilon}\nabla_s\bar{\varphi}_H = \vec{m}\cdot\nabla_s\bar{\varphi}_H \tag{3.7}$$

The subscript affixed to the gradient symbol indicates differentiation with respect to the source coordinates. The distance R from the plumb point of the source at the top of the mantle to the receiver point as defined in eq. (2.73) does not change on vertical variation of the source location. Therefore the derivative of R with respect to the vertical source coordinate vanishes.

3) The gradients in (3.6) and (3.7) require operation on $\bar{\Delta}_V(\zeta)$ and $\bar{\Delta}_H(\zeta)$ defined in eq. (2.46) and (2.47). It should be realized that these two quantities are only dependent on the vertical of the source coordinates, while derivatives with respect to the horizontal source coordinates will vanish. The crustal matrix J (see eq. (2.33)) does not contain the source depth $D = \zeta + z_{s-1}$ as parameter; only the expressions for U and V are ζ dependent, since they

contain the top source matrix $A_{R_{S1}}$ (see eq. 2.34)):

$$A_{R_{S1}} = a_{S1} \cdot a_{S-1} \cdot \ldots\ldots \cdot a_1 \tag{3.8}$$

In this matrix product only the top source layer matrix a_{S1} is ζ dependent. We define the derivative matrix a'_{S1} :

$$a'_{S.} = \frac{\partial}{\partial \zeta}\left(a_{S1}(\zeta)\right) \tag{3.9}$$

and likewise:

$$A'_{R_{S1}} = a'_{S1} \cdot a_{S-1} \cdot \ldots\ldots \cdot a_1 \tag{3.10}$$

or

$$A'_{R_{S1}} = a'_{S1} \cdot A_{R_{S-1}} \tag{3.11}$$

Referring to eq (2.41) and (2.42) for U and V we need only the following elements of $A'_{R_{S1}}$:

$$(A'_{R_{S1}})_{11} \;;\; (A'_{R_{S1}})_{12} \;;\; (A'_{R_{S1}})_{21} \;;\; (A'_{R_{S1}})_{22}$$

The elements of a'_{S1} which will be used for the computation of these 4 elements are (compare eq. (2.16)):

$$\begin{aligned}
(a'_{S1})_{11} &= -k\left[\gamma_s r_{\alpha_s} \sin P_s - (\gamma_s - 1) r_{\beta_s} \sin Q_s\right] \\
(a'_{S1})_{12} &= i k\left[(\gamma_s - 1)\cos P_s + \gamma_s r_{\beta_s}^2 \cos Q_s\right] \\
(a'_{S1})_{13} &= \frac{k}{\rho_s c^2}\left[r_{\alpha_s} \sin P_s - r_{\beta_s} \sin Q_s\right] \\
(a'_{S1})_{14} &= \frac{ik}{\rho_s c^2}\left[\cos P_s + r_{\beta_s}^2 \cos Q_s\right] \\
(a'_{S1})_{21} &= -ik\left[\gamma_s r_{\alpha_s}^2 \cos P_s + (\gamma_s - 1)\cos Q_s\right] \\
(a'_{S1})_{22} &= k\left[(\gamma_s - 1) r_{\alpha_s} \sin P_s - \gamma_s r_{\beta_s} \sin Q_s\right] \\
(a'_{S1})_{23} &= \frac{ik}{\rho_s c^2}\left[r_{\alpha_s}^2 \cos P_s + \cos Q_s\right] \\
(a'_{S1})_{24} &= (a'_{S1})_{13}
\end{aligned} \tag{3.12}$$

The quantities

$$\bar{\Delta}'_V = \frac{\partial}{\partial \zeta} \bar{\Delta}_V \quad \text{and} \quad \bar{\Delta}'_H = \frac{\partial}{\partial \zeta} \bar{\Delta}_H \qquad (3.13)$$

are obtained from $\bar{\Delta}_V$ and $\bar{\Delta}_H$ by simply replacing the elements of the top source layer matrix a_{s1} by those of the derivative matrix a'_{s1}.

4) For handy reference in the following sections we define the following two vector quantities:

$$\vec{V} = \left\{ i k r_{\alpha_n} \cos\theta \, \bar{\Delta}_V , \; i k r_{\alpha_n} \sin\theta \, \bar{\Delta}_V , \; \bar{\Delta}'_V \right\} \qquad (3.14)$$

$$\vec{H} = \left\{ i k r_{\alpha_n} \cos\theta \, \bar{\Delta}_H , \; i k r_{\alpha_n} \sin\theta \, \bar{\Delta}_H , \; \bar{\Delta}'_H \right\} \qquad (3.15)$$

5) The transformed dilatational potential $\bar{\varphi}_\infty$ due to a point force acting in direction $\vec{n}$ in an infinite homogeneous isotropic medium is given by:

$$\bar{\varphi}_\infty = - \frac{\bar{L}}{4\pi \omega^2 \rho_n} \, \vec{n} \cdot \nabla_s \left(\frac{e^{-i k_{\alpha_n} R}}{R} \right) \qquad (3.16)$$

where ρ_n is the density of the infinite medium made up of subcrustal material. At large distances this is:

$$\bar{\varphi}_\infty = - \frac{i k_{\alpha_n} \bar{L}}{4\pi \omega^2 \rho_n} \left(\vec{n} \cdot \vec{R}^0 \right) \frac{e^{-i k_{\alpha_n} R}}{R} \qquad (3.17)$$

Here $\vec{R}^0$ is the unit vector in the direction from source to receiver:

$$\vec{R}^0 \quad \frac{1}{R}\left\{ x, y, z \right\} = \left\{ \cos\gamma \cos\theta, \cos\gamma \sin\theta, \sin\gamma \right\} \qquad (3.18)$$

From $\bar{\varphi}_\infty$ we derive the potential $\bar{\varphi}'_\infty$ due to a couple of forces acting on a line element with direction $\vec{m}$ by determining the component of the gradient of $\bar{\varphi}_\infty$ in the direction $\vec{m}$ (compare eq. (3.6) and (3.7)):

$$\bar{\varphi}'_\infty = \vec{m} \cdot \nabla_s \bar{\varphi}_\infty \tag{3.19}$$

This is for large distances:

$$\bar{\varphi}'_\infty = -\frac{i}{4\pi\alpha_n^2\rho_n} (\vec{n}\cdot\vec{R}^0)(\vec{m}\cdot\vec{R}^0) \frac{e^{-ik_{\alpha_n}R}}{R} \tag{3.20}$$

3.2 The explosive point source.

An explosive point source can be represented by 3 mutual perpendicular couples of equal point forces without moment. In case of the layered medium we will represent the source by one vertical couple in the vertical z-direction and two horizontal couples in the x- and y-direction. The potentials for these couples are obtained by operating with (3.6) and (3.7) on the expressions for $\bar{\varphi}_V$ and $\bar{\varphi}_H$ from eq. (2.81) and (2.83). For the dilatational potential of the vertical couple we obtain at large distances, omitting terms of higher order:

$$\bar{\varphi}'_V(r,z) = -i\left(\frac{\alpha_n}{\omega}\right)^2 r_{\alpha_n} \bar{\Delta}'_V \frac{e^{-ikr_{\alpha_n}}}{R} \tag{3.21}$$

likewise for the sum of the potentials due to the two horizontal couples:

$$\bar{\varphi}'_H(r,z) = i\left(\frac{\alpha_n}{\omega}\right)^2 k r_{\alpha_n} \bar{\Delta}_H \frac{e^{-ikr_{\alpha_n}}}{R} \tag{3.22}$$

Superposing the two potentials $\bar{\varphi}'_V$ and $\bar{\varphi}'_H$ we finally arrive at the dilatational potential $\bar{\varphi}_1$ due to an explosive point

source in a layered medium:

$$\tilde{\varphi}_1(r,z) = -\frac{\bar{L}k}{2\pi}\left(\frac{\alpha_n}{\omega}\right)^2 k r_{\alpha_n}\left[-\frac{i}{k}\bar{\Delta}'_V + i\,\bar{\Delta}_H\right]\frac{e^{-ik_{\alpha_n}R}}{R} \tag{3.23}$$

The same source in the infinite medium of subcrustal material gives rise to the following potential at large distances:

$$\bar{\varphi}_{1\infty}(r,z) = -\frac{\bar{L}}{4\pi\alpha_n^2\rho_n}\,\frac{e^{-ik_{\alpha_n}R}}{R} \tag{3.24}$$

This may be realized from (3.20) by remembering that for all three couples without moment $\vec{n}$ is equal to $\vec{m}$. Thus essentially the following terms have to be summed:

$$\begin{aligned}(\vec{n}_1\cdot\vec{R}^0)^2 + (\vec{n}_2\cdot\vec{R}^0)^2 + (\vec{n}_3\cdot\vec{R}^0) &= \\ = (R^0_1)^2 + (R^0_2)^2 + (R^0_3)^2 &= 1\end{aligned} \tag{3.25}$$

According to (3.1) the transfer function T_1 is then

$$T_1 = 2\alpha_n^2\rho_n \sin\gamma\cos\gamma\left[-\frac{i}{k}\bar{\Delta}'_V + i\,\bar{\Delta}_H\right] \tag{3.26}$$

where use has been made of

$$\sin\gamma = \frac{\alpha_n}{c} \quad \text{and} \quad r_{\alpha_n} = \operatorname{ctg}\gamma = \sqrt{\frac{c^2}{\alpha_n^2} - 1} \tag{3.27}$$

3.3 The single couple type of point source

The single couple type of point source is depicted in figure 4. Without loss of generality we shall choose the x, y, z - system orientation so that the horizontal component of the force is in the direction of the x-axis $(\Theta = 0^\circ)$.

The direction of unit vector $\vec{m}$ along the line element is

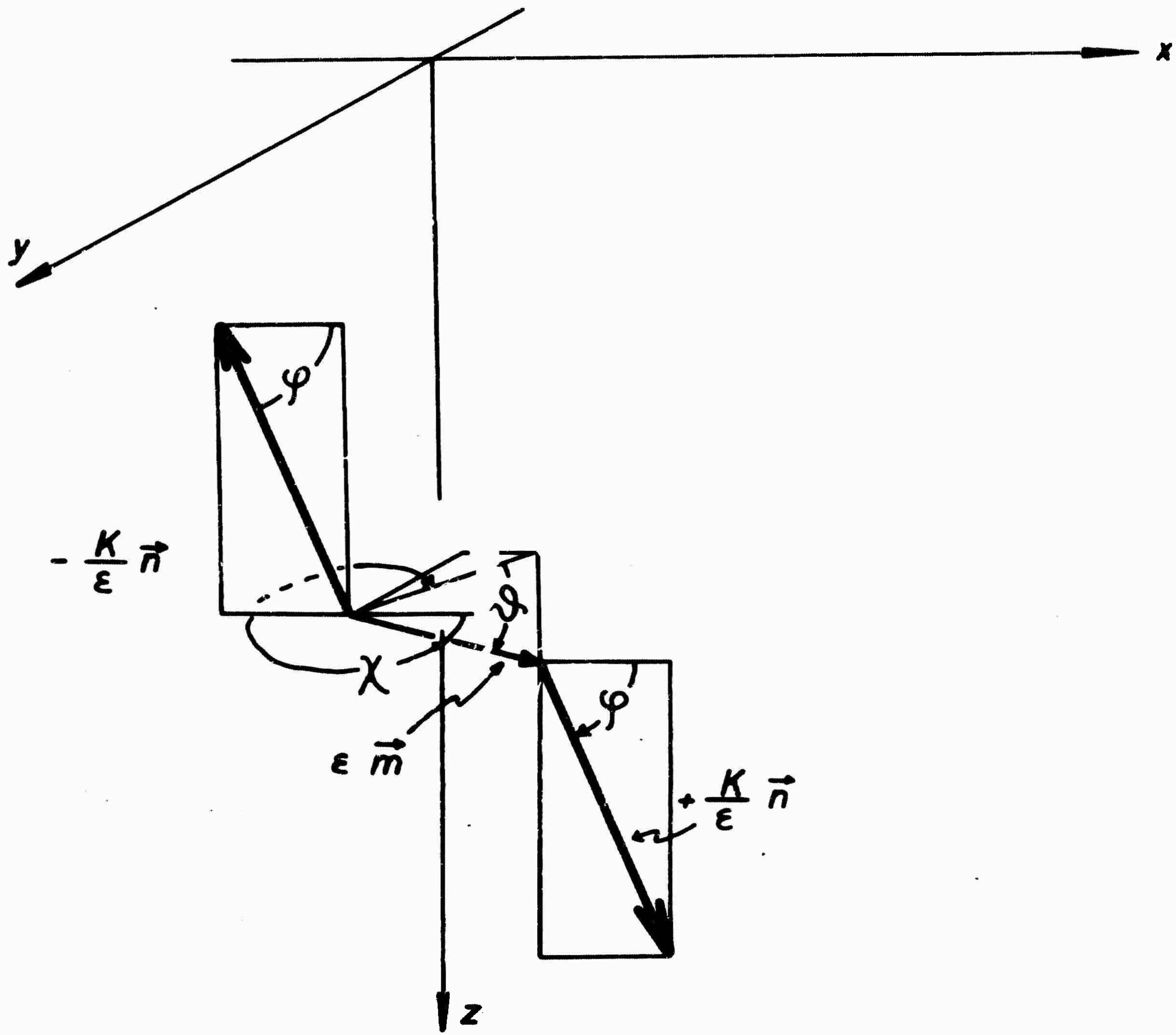
x
y
z
φ
φ
ϑ
χ
$-\frac{K}{\varepsilon}\vec{n}$
$\varepsilon\,\vec{m}$
$+\frac{K}{\varepsilon}\vec{n}$

Fig. 4

arbitrary, the only constraint being that the point force and the line element are perpendicular:

$$\vec{m} \cdot \vec{n} = 0 \tag{3.28}$$

The following notations will be used:

φ : plunge of $\vec{n}$

χ : trend of $\vec{m}$

ϑ : plunge of $\vec{m}$

Thus $\vec{m}$ and $\vec{n}$ have the following components in the xyz-system:

$$\vec{m} = \{\cos\vartheta\cos\chi,\ \cos\vartheta\sin\chi,\ \sin\vartheta\} \tag{3.29}$$

$$\vec{n} = \{\cos\varphi,\ 0,\ \sin\varphi\} \tag{3.30}$$

The constraint (3.28) gives rise to the following relation:

$$\cos\vartheta\cos\chi\cos\varphi + \sin\vartheta\sin\varphi = 0 \tag{3.31}$$

We shall distinguish two cases:

Case A: $\varphi \neq 0^\circ$ or 180° and $\chi \neq 90^\circ$ or 270°

Case B: $\varphi = 0^\circ$ or 180° and $\chi = 90^\circ$ or 270°

For case A relation (3.31) is satisfied if:

$$\cos\vartheta = \frac{\sin\varphi}{\sin\alpha} \tag{3.32}$$

$$\sin\vartheta = -\frac{\cos\varphi\cos\chi}{\sin\alpha} \tag{3.33}$$

where

$$\sin\alpha = \sqrt{1-\sin^2\chi\cos^2\varphi} \neq 0 \tag{3.34}$$

In this case the two unit vectors $\vec{m}$ and $\vec{n}$ have the following components:

$$\vec{m} = \frac{1}{\sin\alpha}\{\sin\varphi\cos\chi,\ \sin\varphi\sin\chi,\ -\cos\varphi\cos\chi\} \tag{3.35}$$

$$\vec{n} = \{\cos\varphi,\ 0,\ \sin\varphi\} \tag{3.36}$$

For case B relation (3.31) is satisfied for arbitrary plunge ϑ of $\vec{m}$. The two unit vectors then become:

$$\vec{m} = \{0,\ \cos\vartheta,\ \sin\vartheta\} \tag{3.37}$$

$$\vec{n} = \{1,\ 0,\ 0\} \tag{3.38}$$

Referring to the remarks on the decomposition of force couples in section 3.1 and applying eq. (3.6) and (3.7) to the potential of the vertical and horizontal component forces, we find for the dilatational potentials $\bar{\varphi}'_{2V}$ and $\bar{\varphi}'_{2H}$ at large distances.

$$\bar{\varphi}'_{2V}(r,\theta,z) = +\frac{Lk}{2\pi}\, i\left(\frac{\alpha_n}{\omega}\right)^2 r_{\alpha_n}\sin\varphi\,(\vec{m}\cdot\vec{V})\,\frac{e^{-ik_{\alpha_n}R}}{R}. \tag{3.39}$$

$$\bar{\varphi}'_{2H}(r,\theta,z) = -\frac{Lk}{2\pi}\left(\frac{\alpha_n}{\omega}\right)^2 r_{\alpha_n}\cos\varphi\cos\theta\,(\vec{m}\,\vec{H})\,\frac{e^{-ik_{\alpha_n}R}}{R} \tag{3.40}$$

Here $\vec{V}$ and $\vec{H}$ are the vectors defined in (3.14) and (3.15). The sum of both potentials is the dilatational potential of a point source of the single couple type in a layered

medium:

$$\bar{\varphi}_2(r,\theta,z) = -\frac{\bar{L}k}{2\pi}\left(\frac{a_n}{\omega}\right)^2 r_{a_n}\left[-i\sin\varphi(\vec{m}\cdot\vec{V})+\cos\varphi\cos\Theta(\vec{m}\cdot\vec{H})\right]\frac{e^{-ik_{a_n}R}}{R} \qquad (3.41)$$

The same source in the infinite medium of subcrustal material produces the following dilatational potential (see eq. (3.20)):

$$\bar{\varphi}_{2\infty}(r,\theta,z) = -\frac{\bar{L}}{4\pi a_n^2 \rho_n}(\vec{n}\cdot\vec{R}^0)(\vec{m}\cdot\vec{R}^0)\frac{e^{-ik_{a_n}R}}{R} \qquad (3.42)$$

From eq. (3.1) the transfer function T_2 is:

$$T_2 = 2\,\frac{a_n^4 \rho_n k r_{a_n}}{\omega^2}\,\frac{[-i\sin\varphi(\vec{m}\cdot\vec{V})+\cos\varphi\cos\Theta(\vec{m}\cdot\vec{H})]}{(\vec{n}\cdot\vec{R}^0)(\vec{m}\cdot\vec{R}^0)} \qquad (3.43)$$

3.4 The double couple type of point source

The so-called double couple type of point source is equivalent to a pair of tension and pressure couples without moment (see e.g. Stauder, 1962). We shall denote the unit vector in the direction of tension by $\vec{t}$, and the unit vector in the direction of pressure by $\vec{p}$. Both are mutually perpendicular:

$$\vec{t}\cdot\vec{p} = 0 \qquad (3.44)$$

Without loss of generality we will choose our x,y,z system so that the tension couple is always in the x,z -plane. The plunge of $\vec{t}$ is denoted by φ, therefore:

$$\vec{t} = \{\cos\varphi,\ 0,\ \sin\varphi\} \qquad (3.45)$$

The orientation of $\vec{n}$ will be described by its plunge ϑ and its trend χ :

$$\vec{p} = \{\cos\vartheta\cos\chi,\ \cos\vartheta\sin\chi,\ \sin\vartheta\} \qquad (3.46)$$

The constraint (3.44) gives rise to the same relation as in eq. (3.31). As in the previous case we must distinquish case A and case B.

Case A: $\varphi \neq 0^\circ$ or $\neq 180^\circ$, $\chi \neq 90^\circ$ or 270°

$$\vec{p} = \frac{1}{\sin\alpha}\{\sin\varphi\cos\chi,\ \sin\varphi\sin\chi,\ -\cos\varphi\cos\chi\} \tag{3.47}$$

$$\vec{t} = \{\cos\varphi,\ 0,\ \sin\varphi\} \tag{3.48}$$

where $\sin\alpha$ is the same as in eq. (3.34)

Case B: $\varphi = 0^\circ$ or 180°; $\chi = 90^\circ$ or 270°

$$\vec{p} = \{0,\ \cos\vartheta,\ \sin\vartheta\} \tag{3.49}$$

$$\vec{t} = \{1,\ 0,\ 0\} \tag{3.50}$$

By the same method as in the previous section we derive the potentials due to the vertical and the horizontal components of the tension couple from:

$$\bar{\varphi}'_{tV} = \vec{t}\cdot\nabla_s\left[-i\left(\frac{a_n}{\omega}\right)^2 r_{an}\bar{\Delta}_V\frac{e^{-ik_{an}R}}{R}\sin\varphi\left(-\frac{\bar{L}k}{2\pi}\right)\right] \tag{3.51}$$

and

$$\bar{\varphi}'_{tH} = \vec{t}\cdot\nabla_s\left[\left(\frac{a_n}{\omega}\right)^2 r_{an}\bar{\Delta}_H\cos\Theta\,\frac{e^{-ik_{an}R}}{R}\cos\varphi\left(-\frac{\bar{L}k}{2\pi}\right)\right] \tag{3.52}$$

For large $k_{an}R \gg 1$ we neglect higher order terms of the gradient

$$\bar{\varphi}'_{tV} = i\left(\frac{a_n}{\omega}\right)^2 r_{an}\sin\varphi\,\frac{\bar{L}k}{2\pi}\,(\vec{t}\cdot\vec{V})\,\frac{e^{-ik_{an}R}}{R} \tag{3.53}$$

$$\bar{\varphi}'_{tH} = -\left(\frac{a_n}{\omega}\right)^2 r_{an}\cos\varphi\,\frac{\bar{L}k}{2\pi}\cos\Theta\,(\vec{t}\cdot\vec{H})\,\frac{e^{-ik_{an}R}}{R} \tag{3.54}$$

$\vec{V}$ and $\vec{H}$ are again defined in eq. (3.14) and (3.15).

In the same manner we derive the potential due to the vertical

component of the pressure couple:

$$\bar{\varphi}'_{pv} = -i \left(\frac{d_n}{\omega}\right)^2 r_{\alpha_n} p_3 \frac{\bar{L} k}{2\pi} (\vec{p} \cdot \vec{V}) \frac{e^{-i k_{\alpha_n} R}}{R} \tag{3.55}$$

where p_3 is the z-component of $\vec{p}$, eq. (3.47) or (3.49).

The two potentials due to the x- and y-component of the pressure couple are:

$$\bar{\varphi}'_{px} = \left(\frac{d_n}{\omega}\right)^2 r_{\alpha_n} p_1 \frac{\bar{L} k}{2\pi} \cos\Theta \, (\vec{n} \cdot \vec{H}) \frac{e^{-i k_{\alpha_n} R}}{R} \tag{3.56}$$

$$\bar{\varphi}'_{py} = \left(\frac{d_n}{\omega}\right)^2 r_{\alpha_n} p_2 \frac{\bar{L} k}{2\pi} \sin\Theta \, (\vec{n} \cdot \vec{H}) \frac{e^{-i k_{\alpha_n} R}}{R} \tag{3.57}$$

Both potentials $\bar{\varphi}'_{px}$ and $\bar{\varphi}'_{py}$ can be combined. This gives in <u>case A</u>:

$$\bar{\varphi}'_{pH} = \bar{\varphi}'_{px} + \bar{\varphi}'_{py} = \left(\frac{d_n}{\omega}\right)^2 r_{\alpha_n} \frac{\sin\varphi}{\sin\alpha} \cos(\chi - \Theta) \frac{\bar{L} k}{2\pi} (\vec{p} \cdot \vec{H}) \frac{e^{-i k_{\alpha_n} R}}{R} \tag{3.58}$$

and the potential $\bar{\varphi}'_{pv}$ is in this case:

$$\bar{\varphi}'_{pv} = +i \left(\frac{d_n}{\omega}\right)^2 r_{\alpha_n} \frac{\cos\varphi \cos\chi}{\sin\alpha} \frac{\bar{L} k}{2\pi} (\vec{p} \cdot \vec{V}) \frac{e^{-i k_{\alpha_n} R}}{R} \tag{3.59}$$

and in <u>case B</u>:

$$\bar{\varphi}'_{pH} = \pm \left(\frac{d_n}{\omega}\right)^2 r_{\alpha_n} \cos\vartheta \sin\Theta \frac{\bar{L} k}{2\pi} (\vec{p} \cdot \vec{H}) \frac{e^{-i k_{\alpha_n} R}}{R} \tag{3.60}$$

$$\bar{\varphi}'_{pv} = -i \left(\frac{d_n}{\omega}\right)^2 r_{\alpha_n} \sin\vartheta \frac{\bar{L} k}{2\pi} (\vec{p} \cdot \vec{V}) \frac{e^{-i k_{\alpha_n} R}}{R} \tag{3.61}$$

The resultant dilatational potential $\bar{\varphi}_3$ of the double couple is the sum of four potentials:

$$\bar{\varphi}_3 = \bar{\varphi}'_{tv} + \bar{\varphi}'_{tH} + \bar{\varphi}'_{pv} + \bar{\varphi}'_{pH} \tag{3.62}$$

We distinguish again the two cases A and B.

Case A: With eq. (3.53), (3.54), (3.58), and (3.59) we derive:

$$\bar{\varphi}_3(r,\Theta,z) = \left(\frac{\alpha_n}{\omega}\right)^2 r_{\alpha_n} \frac{\bar{L}k}{2\pi}\Big[i\sin\varphi(\vec{t}\cdot\vec{V}) + i\frac{\cos\varphi\cos\chi}{\sin\alpha}(\vec{p}\cdot\vec{V}) - \cos\varphi\cos\Theta(\vec{t}\cdot\vec{H}) + \frac{\sin\varphi}{\sin\alpha}\cos(\chi-\Theta)(\vec{p}\cdot\vec{H})\Big]\frac{e^{-ik_{\alpha_n}R}}{R} \tag{3.63}$$

Case B: From eq. (3.53), (3.54), (3.60) and (3.61)

$$\bar{\varphi}_3(r,\Theta,z) = \left(\frac{\alpha_n}{\omega}\right)^2 r_{\alpha_n} \frac{\bar{L}k}{2\pi}\Big[-i\sin\vartheta(\vec{p}\cdot\vec{V}) - \cos\Theta(\vec{t}\cdot\vec{H}) + \cos\vartheta\sin\Theta(\vec{p}\cdot\vec{H})\Big]\frac{e^{-ik_{\alpha_n}R}}{R} \tag{3.64}$$

The same double couple source in the infinite medium of subcrustal material produces the following dilatational potential $\bar{\varphi}_{3\infty}$:

$$\bar{\varphi}_{3\infty} = \frac{\bar{L}}{4\pi\alpha_n^2\rho_n}\Big[(\vec{p}\cdot\vec{R}^0)^2 - (\vec{t}\cdot\vec{R}^0)^2\Big]\frac{e^{-ik_{\alpha_n}R}}{R} \tag{3.65}$$

(3.65) is derived according to (3.20) by summing the effect of the tension and of the pressure couple. The transfer function T_3 is derived with (3.1). Distinguishing the two cases we find:

Case A:

$$T_3 = 2\frac{\alpha_n^4\rho_n}{\omega^2}\frac{k r_{\alpha_n}}{} \cdot \frac{\Big[i\sin\varphi(\vec{t}\cdot\vec{V}) + i\frac{\cos\varphi\cos\chi}{\sin\alpha}(\vec{p}\cdot\vec{V}) - \cos\varphi\cos\Theta(\vec{t}\cdot\vec{H}) + \frac{\sin\varphi}{\sin\alpha}\cos(\chi-\Theta)(\vec{p}\cdot\vec{H})\Big]}{(\vec{p}\cdot\vec{R}^0)^2 - (\vec{t}\cdot\vec{R}^0)^2} \tag{3.66}$$

Case B:

$$T_3 = \frac{2\alpha_n^4 g_n k r_{\alpha n}}{\omega^2} \frac{\left[-i\sin\vartheta(\vec{p}\cdot\vec{V}) - \cos\Theta(\vec{t}\cdot\vec{H}) + \cos\vartheta\sin\vartheta(\vec{p}\cdot\vec{H})\right]}{(\vec{p}\cdot\vec{R^0})^2 - (\vec{t}\cdot\vec{R^0})^2} \qquad (3.67)$$

3.5 Remark on nodal planes

The single and double couple type of point source in the infinite medium have nodal planes where the potential vanish. These nodal planes are defined by:

a) Single couple (see eq. (3.42)):

$$(\vec{n}\cdot\vec{R^0})(\vec{m}\cdot\vec{R^0}) = 0 \qquad (3.68)$$

that is

$$\vec{n}\cdot\vec{R^0} = 0 \; ; \quad \vec{m}\cdot\vec{R^0} = 0 \qquad (3.69)$$

The potentials are zero in planes normal to $\vec{n}$ (the direction of the force) and normal to $\vec{m}$ (the direction of the line element).

b) Double couple (see eq. (3.65)):

$$(\vec{p}\cdot\vec{R^0})^2 = (\vec{t}\cdot\vec{R^0})^2 \qquad (3.70)$$

This is fulfilled if:

$$\vec{p}\cdot\vec{R^0} = \pm\,\vec{t}\cdot\vec{R^0} \qquad (3.71)$$

or

$$(\vec{p} \mp \vec{t})\cdot\vec{R^0} = 0 \qquad (3.72)$$

Since $\vec{p}$ and $\vec{t}$ are unit vectors their sum and their difference form vectors in the direction of bisecting lines between the pressure and the tension couple. (3.72) states that the potential vanishes in the planes normal to these two bisecting lines.

On these nodal planes the present definition of the transfer function T_2 and T_3 in eq. (3.43) and (3.66) and (3.67) lose their meaning, since here the denominator becomes zero. In general it cannot be expected that the nodal planes of the source in the infinite medium do coincide with the nodal planes for the point source in the crust. We will by-pass this problem by defining modified transfer functions $\tilde{T}_2$ and $\tilde{T}_3$:

$$\tilde{T}_2 = (\vec{n}\cdot\vec{R^0})(\vec{m}\cdot\vec{R^0})\ T_2$$

and

$$\tilde{T}_3 = \left[(\vec{p}\cdot\vec{R^0})^2 - (\vec{t}\cdot\vec{R^0})^2\right]\ T_3$$

These modified transfer functions will not "blow up" on the nodal planes.

The explosive point source in the infinite medium does not display any nodal lines. Therefore there is no necessity of defining a modified transfer function in that case.

4.0 Preliminary numerical computations for the transfer function of an explosive point source.

4.1 Introduction

The transfer functions T_1, T_2 and T_3 (or $\tilde{T}_2$ and $\tilde{T}_3$) are given in a form which is convenient for programming for automatic computations. The three functions have been programmed in IBM Fortran II for the IBM 7072. The transfer functions contain not only the parameters of the source in the infinite medium but also:

a) the parameters of the crustal model:

$$\alpha_i ,\ \beta_i ,\ \rho_i \qquad\qquad i = 1, \dots, n$$

d_i, the layer thicknesses,

b) The depth ζ of the source in the source layer

c) The angle of incidence γ into the mantle.

In this paper we will only give preliminary numerical results for the explosive point source as the simplest type. There is no azimuthal dependence; no nodal planes exist for the source in the infinite medium. The selected examples are not considered to be complete, but they will serve as guide to further detailed computation.

Even in the case of the explosive source we will confine ourselves to the study of the following questions:

1) Given a standard crustal model, how does the source depth influence the transfer function?

2) For a fixed source depth in the standard model, how does the transfer function vary with the angle of incidence γ ?

3) How do minor variations of the standard model influence the transfer function?

The program for the transfer function T_1 is based on eq. (3.26) in section 3.2. For the computation of $\bar{\Delta}'_v$ and Δ_μ the elements of the crustal matrix J, eq. (2.33), and the quantities U and V, eq.(2.41) and (2.42) must be determined. With some minor modifications the program uses the same techniques of multiplication of matrices with real and imaginary elements as that of Hannon (1964a,b).

The program has been tested in the case of an explosive point source by comparing the theoretically known response to a δ-excitation for the point source in a homogeneous half-space with the response, calculated from the source-crust transfer function T , by Fourier synthesis, of a layered model in which all layers have identical properties. For the models used in this section the program has been run for a frequency range 0 to 5 cps without "blowing up."

4.2 The influence of the angle of incidence γ.

We will place the explosive point source at a fixed depth of 30 km in a standard crustal model, the same as used by Van Nostrand (1964):

Table 1: Standard Crust NCCR

Depth interval (km)	P- (km/sec)	S-Velocity (km/sec)	Density (g/cm^3)
0 - 3	3.10	1.79	2.35
3 - 20	6.03	3.48	2.60
20 - 45	6.97	4.02	3.00
45 - ∞	8.10	4.67	3.35

The crustal model is displayed on the right-hand side of figure 5. The amplitudes of the transfer functions have been determined for the following angles of incidence: $\gamma = 15^\circ, 30^\circ, 45^\circ, 60^\circ, 75^\circ$. The values of the corresponding horizontal phase velocities c are indicated in the figure. It may be concluded that the spectra of P-waves incident into the mantle at various angles do not vary sig-

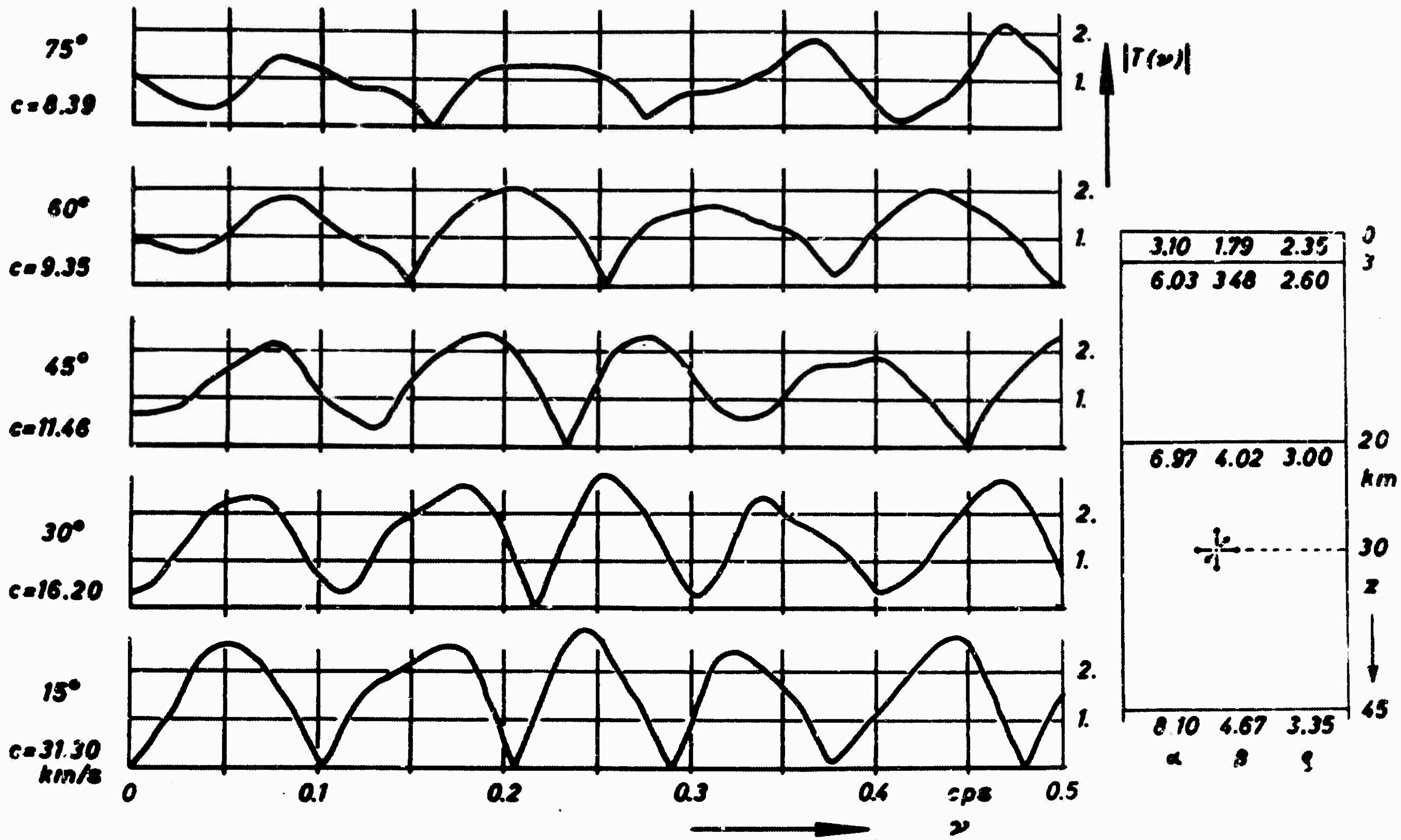

AMPLITUDE of TRANSFER FUNCTION
EXPLOSIVE SOURCE CRUST SYSTEM

Fig 5

nificantly with angle of incidence in a frequency range from 0 to about 0.3 cps. This is especially true for angles of incidence between 15° and 45°. The first peak at 0.05 cps and the first trough at 0.1 cps can be attributed to constructive and destructive interference between the direct P-wave and the pP reflection from the free surface. In this part of the spectrum the transfer function is predominantly governed by the interference between P and pP waves. The fine structure of the crust has practically no influence on the spectrum. The slight shift of peaks and troughs towards higher frequencies at increasing angle of incidence may be accounted for by decreasing time lags of reflections within the crust.

4.3 The influence of the source depth

Using the same crustal model as in figure 5 we will now place the source at three different depths: 0.5, 8.0 and 30.0 km. The angle of incidence into the mantle is chosen as $\gamma = 45^{\circ}$. The amplitude of the transfer functions are displayed in figure 6 for the frequency range 0 to 0.3 cps. For a source depth of 0.5 km the first peak due to constructive P and pP interference should occur at 1.6 cps. Therefore $|T|$ is relatively flat up to about 0.2 cps. This becomes clear on comparison with $|T|$ for 8.0 km depth and 30 km depth where the first peaks are located at 0.2 cps and 0.07 cps, respectively.

It may be concluded that the transfer function for an explosive source in a crust is rather sensitive to changes in the depth of the source. This becomes even more evident

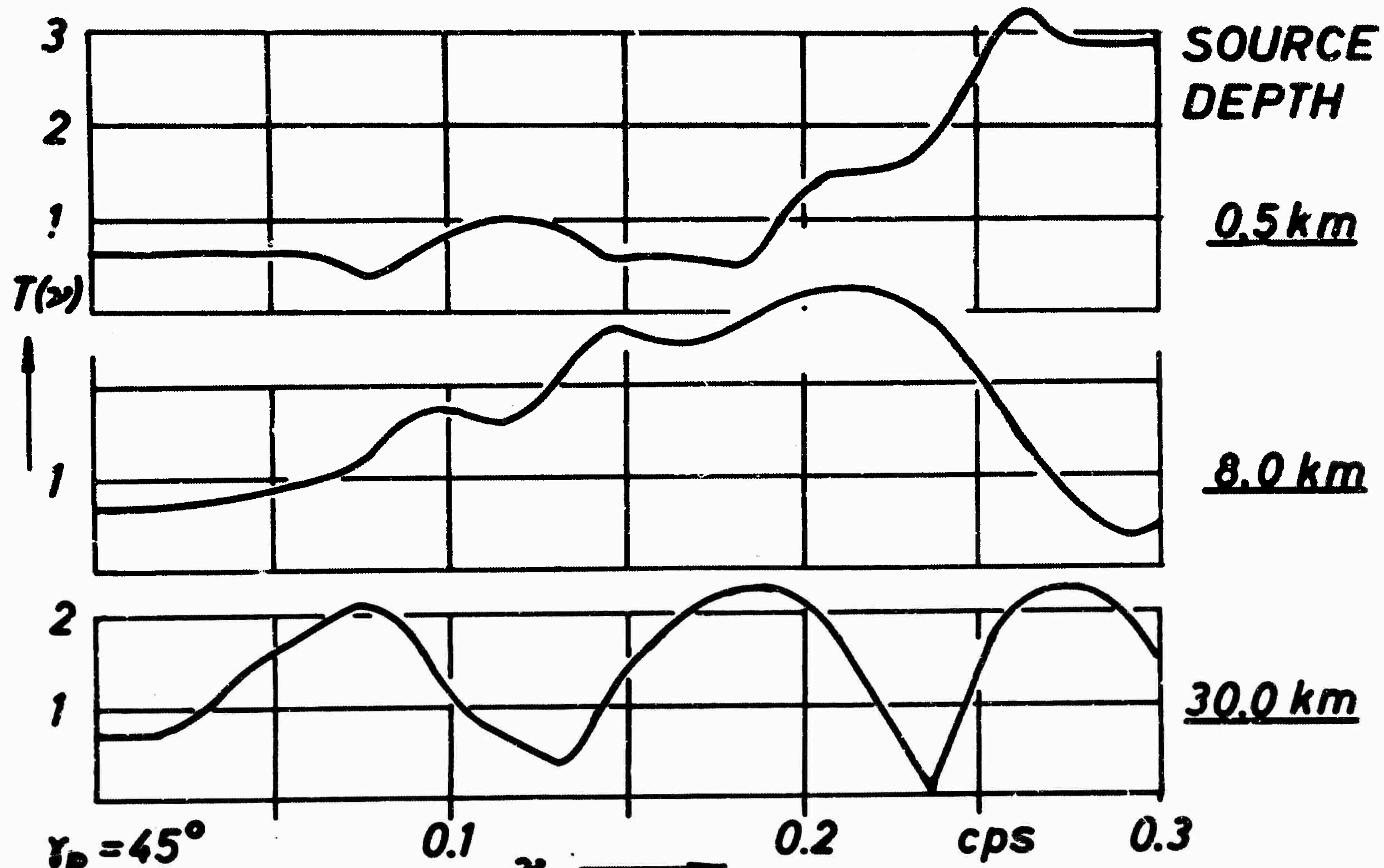

AMPLITUDE of TRANSFER FUNCTION
EXPLOSIVE SOURCE CRUST SYSTEM

if one considers the spectrum up to 4 cps.

In figures 7 and 8 the amplitude $|T|$ and the phase δ of T is depicted for two source depths: 0.5 and 8.0 km for $\gamma = 45^{\circ}$. Note especially the very high amplitudes for the near surface source between 1.2 and 2.0 cps, and the relatively low amplitudes for very low frequencies between 0 and 0.2 cps and the band between 3.0 and 3.4 cps. Comparing this with the spectrum of the deeper source one may draw the following tentative conclusions:

As the source moves closer to the free surface the low frequency part of the transfer function becomes a band of relatively low amplitudes compared to the amplitudes of the higher frequency bands; e.g. for a point source at 0.5 km depth in the standard model NOCR, the average amplitude between 0.0 and 0.3 cps is about 1/5 of the average amplitude in the interval 1.2 and 1.5 cps. In this case the system acts effectively as a rejection filter for the lower frequencies. The closer to the surface the source is located - without violating the free surface condition - the broader is this rejection band. This range of small amplitudes is rather flat compared to the spectrum for the same range of frequencies for a source at larger depths.

Figures 7 and 8 contain also the phase spectrum. It should be noted that troughs in the amplitude spectrum usually coincide with irregular variations in the phase spectrum.

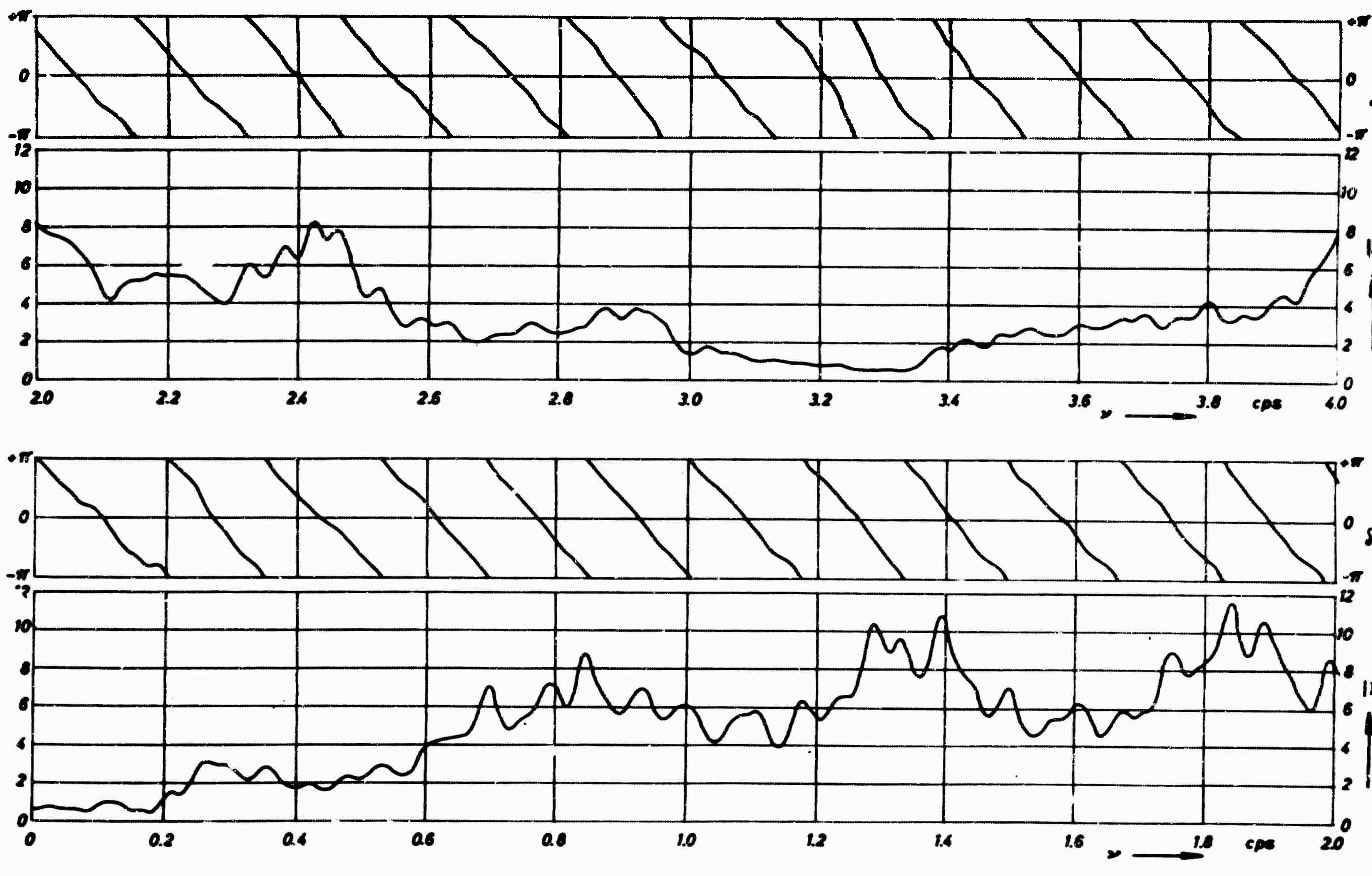

+π
0
-π
δ
12
10
8
6
4
2
0
|T|
2.0
2.2
2.4
2.6
2.8
3.0
3.2
3.4
3.6
3.8
4.0
ν
cps
0
0.2
0.4
0.6
0.8
1.0
1.2
1.4
1.6
1.8
2.0

Fig 7

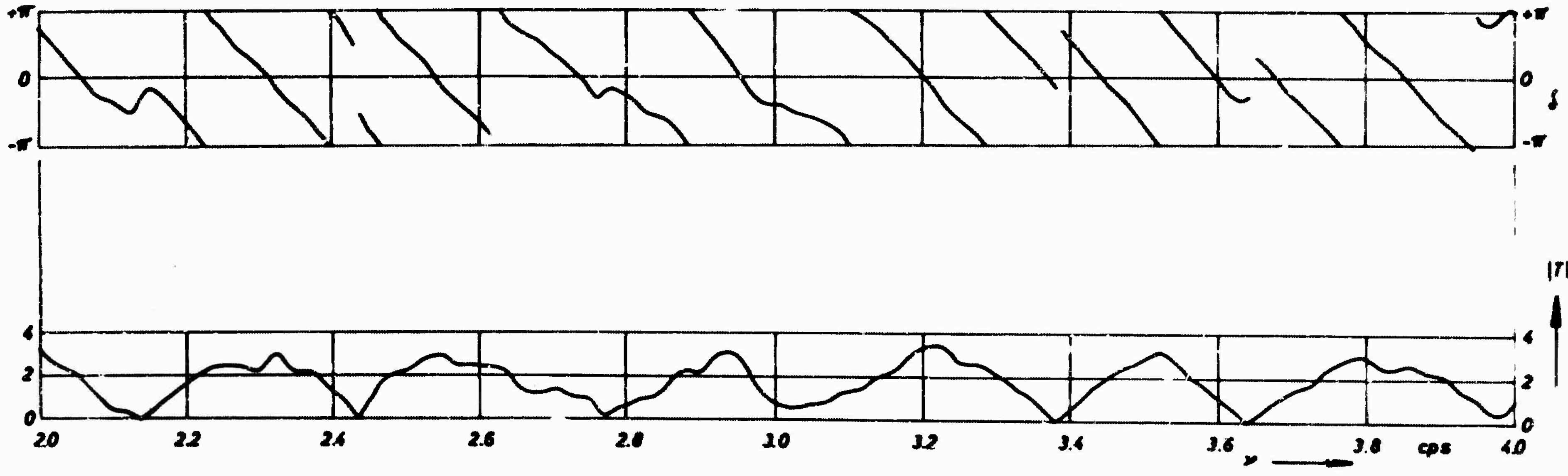

+π
0
-π
δ
|T|
4
2
0
2.0
2.2
2.4
2.6
2.8
3.0
3.2
3.4
3.6
3.8
cps
4.0
ν

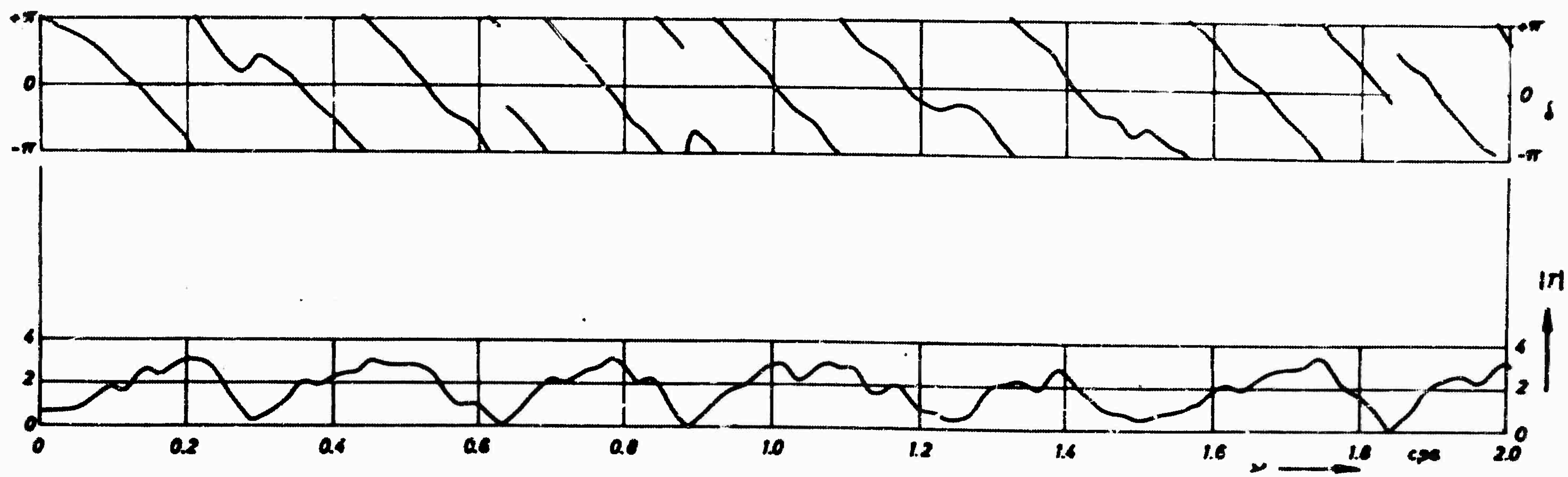

+π
0
-π
δ
|T|
4
2
0
0.2
0.4
0.6
0.8
1.0
1.2
1.4
1.6
1.8
cps
2.0
ν

Fig. 8

4.4 The influence of minor variations of the crustal model

To get an estimate on how minor changes of the crustal model might influence the transfer function, variations have been introduced into the standard model NOCR (see table 1). The models LVC1 and LVC2 are given in tables 2 and 3.

Table 2: Crustal Model LVCI

Depth interval (km)	P- (km/sec)	S-Velocity (km/sec)	Density (g/cm^3)
0 - 3	3.10	1.79	2.35
3 - 6	5.95	3.44	2 65
6 -11	5.50	3.30	2.70
11 - 20	6.03	3.48	2.60
20 - 45	6.97	4.02	3.00
45 - ∞	8.10	4.67	3.35

Table 3: Crustal Model LVC2

Depth interval (km)	P- (km/sec)	S-Velocity (km/sec)	Density (g/cm^3)
0 - 3	3.10	1.79	2.35
3 - 6	5.95	3.44	2.65
6 - 11	5.00	2.90	2.50
11 - 20	6.03	3.48	2.60
20 - 45	6.97	4.02	3.00
45 - ∞	8.10	4.67	3.35

In both models a low velocity channel has been introduced with thickness of 5.0 km. The velocity in the LVC 2 channel is lower than in the LVC1 channel thus increasing the velocity contrast. In figure 9 a comparison between the transfer

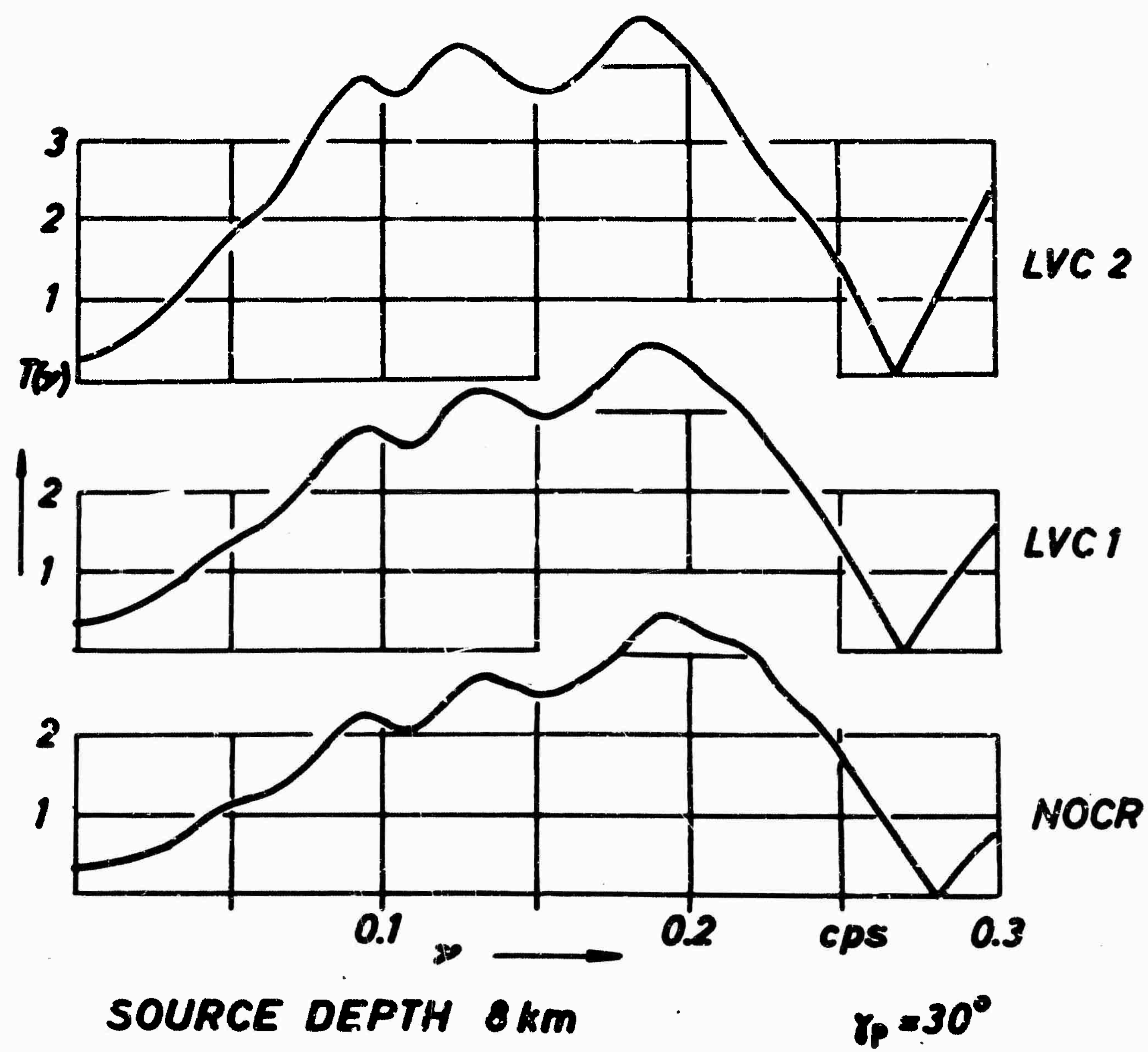

AMPLITUDE of TRANSFER FUNCTION
EXPLOSIVE SOURCE CRUST SYSTEM

Fig 9.

functions of the models NOCR, LVC1 and LVC2 in the frequency range 0 to 0.3 cps is presented. The source has been kept at a depth of 8.0 km for the three models so that for LVC1 and LVC2 the source is located in the low velocity channel. The angle of incidence is $\gamma = 30^{\circ}$. Figure 9 merely demonstrates that in this range of frequency the minor variations so introduced in the model are virtually of no effect on the transfer function. Closer examination shows small differences which, however, would have no significance in signal analysis. In the frequency range greater than about 1 cps differences in the transfer function begin to become noticeable. From the analysis of these and other numerical examples the following might be concluded about the influence of minor variations in the crust:

Minor variations in the crust become significantly apparent in the transfer function only:

1) if the velocity contrast of the newly introduced layer is sufficiently large.
2) if 1) is fulfilled, only that part of the spectrum will be affected above a frequency ν_0, where ν_0 is about the fundamental frequency of "destructive" interference between reflected waves in the new layer.

5.0 Conclusions

Analytical expressions for the transfer functions for dilatational body waves radiating into the mantle from a system consisting of a point source in a layered crust have

been established for large distances. Three types of point sources have been treated: an explosive source, a single couple, and a double couple.

Preliminary numerical calculations of the transfer function for explosive point sources have been presented. They show as especially important features the strong influence of the source depth on the shape of the spectrum and the relatively strong rejection of low frequencies for shallow explosions.

Further analysis of other models, especially of the other two point source types must show to what extent the present conclusions may be generalized.

Acknowledgments

The author wishes to express his personal gratitude to the Rev. William Stauder, S.J., for his continuing interest in this work and stimulating discussions, as well as his assistance in the preparation of this paper. The research reported in this paper was sponsored in part by the Air Force Office of Scientific Research under Grant AF-AFOSR 386-63 and in part by the Air Force Cambridge Research Laboratories, OAR, under Contract AF 19(604)-7399, both for the Advanced Research Projects Agencies' Project VELA-Uniform. Computer computations were partially supported by the Washington University computing facilities through NSF Grant G-22296.

References

Ben-Menahem, A., S. W. Smith, T. Teng
1965 A procedure for source studies from spectrums of long-period seismic body-waves. Bull. Seism. Soc. Am., Vol. 55 (2), pp. 203-235.

Bortfeld, R.
1964 Synthetic records for point sources in arbitrary layered media. Theory and discussion on inhomogeneous sources. Communication on 26th EAEG meeting, 8-11, Dec. 1964, Pau/France.

Dunkin, J. W.
1965 Computation of modal solutions in layered, elastic media at high frequencies. Bull. Seism. Soc. Am., Vol. 55 (2), pp. 335-358.

Ewing, W. M., W. S. Jardetzky, F. Press
1957 Elastic waves in layered Media. McGraw Hill, N.Y., 380 p.

Hannon, W. J.
1964a Some effects of a layered system on dilatational waves. Techn. Report AF Cambridge Research Laborat., Bedford, Mass., Rpt. No. AFCRL 64-614, 68 p.

Hannon, W. J.
1964b An application of the Haskell-Thomson matrix method to the synthesis of the surface motion due to dilatational waves. Bull. Seism. Soc. Am., Vol. 54 (6A), pp. 2067-2079.

Harkrider, D.G.
1964 Surface waves in multilayered elastic media. I. Rayleigh and Love waves from buried sources in a multilayered elastic half-space. Bull. Seism. Soc. Am., Vol. 54 (2), pp. 627-679.

Haskell, N. A.
1953 The dispersion of surface waves on multilayered media. Bull. Seism. Soc. Am., Vol. 43, pp. 17-34.

Jardetzky, W. S.
1953 Period equation for an n-layered half-space and some related questions. Columbia Univ. Lamont Geol. Obs. Techn. Rept. Seismology No. 29, 21 p.

Keylis-Borok, V.L.
1953 Interference seismic waves in a layered medium. Thesis, Inst. of Physics of the Earth, Acad. Sci. USSR.

Nakano, H.
1923 Ncte on the nature of forces which give rise to the earthquake motion. Seism. Bull., Centr. Meteorol. Obs. Japan, Vol. 1, pp. 92-130.

Phinney, R. A.
1964 Structure of the Earth's crust from spectral behavior of long-period body waves. J. Geophys. Res., Vol. 69 (14), pp. 2997-3017.

Stauder, W.
1962 The focal mechanism of earthquakes. Adv. in Geophys., Vol. 9, Acad. Press, N.Y., pp. 1-76.

Thomson, W. T.
1950 Transmission of elastic waves through a stratified medium. J. Appl. Phys., Vol. 21, pp. 89-93.

Van Nostrand, R.
1964 Synthetic earthquake seismograms for teleseismic distances. United ElectroDynamics, Seismic Data Laboratory Report No. 104, Contract AF 33(657)-12447 VT/2037, 10 p.

Unclassified
Security Classification

DOCUMENT CONTROL DATA - R&D

(Security classification of title, body of abstract and indexing annotation must be entered when the overall report is classified)

1. ORIGINATING ACTIVITY (Corporate author) Saint Louis University St. Louis, Missouri	2a. REPORT SECURITY CLASSIFICATION Unclassified 2b. GROUP

3. REPORT TITLE
THE TRANSFER FUNCTION FOR P-WAVES FOR A SYSTEM CONSISTING OF A POINT SOURCE IN A LAYERED MEDIUM

4. DESCRIPTIVE NOTES (Type of report and inclusive dates)
Scientific Report

5. AUTHOR(S) (Last name, first name, initial)
Fuchs, Karl

6. REPORT DATE	7a. TOTAL NO. OF PAGES	7b. NO. OF REFS
July 1965	48 w/9 figures	15

8a. CONTRACT OR GRANT NO. AF 19(604)-7399 ARPA Order No. 292, Project No. 8100, Task 2 b. PROJECT ~~NO.~~ and Task Nos. 865201 c. ~~XXXX~~ d. DOD Element No. 62506015 DOD Subelement No. None	9a. ORIGINATOR'S REPORT NUMBER(S) Scientific Report #[illegible] 9b. OTHER REPORT NO(S) (Any other numbers that may be assigned this report) AFCRL-65-526

10. AVAILABILITY/LIMITATION NOTICES Qualified requestors may obtain copies of this report from DDC. Other persons or organizations should apply to the Clearinghouse for Federal Scientific and Technical Information (CFSTI), Sills Building, 5285 Port Royal Road, Springfield, Va., 22151.

11. SUPPLEMENTARY NOTES	12. SPONSORING MILITARY ACTIVITY Hq. AFCRL, OAR (CRJ) United States Air Force L.G.Hanscom Field, Bedford,Mass.

13. ABSTRACT
This paper investigates in what manner the spectrum of body waves radiating from point sources in a multilayered medium over a homogeneous half-space is different from the spectrum of body waves from the same source in an infinite medium. The effect of the system consisting of a point source in a layered crust on the spectrum of p-waves observed at large distances in the half space is studied. Analytical expressions for the transfer function of this system are derived for three types of point sources: an explosive source, a single couple, and a double couple of arbitrary orientation within the crust.

Preliminary numerical computations for the explosive source at various depths in a realistic model of the earth's crust study the effect of: a) the angle of incidence into the homogeneous half-space, b) the source depth, c) minor variations of the crustal model. In the case of an explosive source the most influential parameter of the transfer function is the source depth. In shallow explosions the low frequency part of the spectrum of body waves is comparatively rejected.

DD FORM 1 JAN 64 1473

Unclassified
Security Classification

14. KEY WORDS	LINK A ROLE	LINK A WT	LINK B ROLE	LINK B WT	LINK C ROLE	LINK C WT
Transfer Function						
Layered Crust						
Depth of Focus						
Point Source in Crust						
Filter Properties of Crust						
P Wave						
Focal Mechanism						

INSTRUCTIONS

1. ORIGINATING ACTIVITY: Enter the name and address of the contractor, subcontractor, grantee, Department of Defense activity or other organization *(corporate author)* issuing the report.

2*a*. REPORT SECURITY CLASSIFICATION: Enter the overall security classification of the report. Indicate whether "Restricted Data" is included. Marking is to be in accordance with appropriate security regulations.

2*b*. GROUP: Automatic downgrading is specified in DoD Directive 5200.10 and Armed Forces Industrial Manual. Enter the group number. Also, when applicable, show that optional markings have been used for Group 3 and Group 4 as authorized.

3. REPORT TITLE: Enter the complete report title in all capital letters. Titles in all cases should be unclassified. If a meaningful title cannot be selected without classification, show title classification in all capitals in parenthesis immediately following the title.

4. DESCRIPTIVE NOTES: If appropriate, enter the type of report, e.g., interim, progress, summary, annual, or final. Give the inclusive dates when a specific reporting period is covered.

5. AUTHOR(S): Enter the name(s) of author(s) as shown on or in the report. Enter last name, first name, middle initial. If military, show rank and branch of service. The name of the principal author is an absolute minimum requirement.

6. REPORT DATE: Enter the date of the report as day, month, year, or month, year. If more than one date appears on the report, use date of publication.

7*a*. TOTAL NUMBER OF PAGES: The total page count should follow normal pagination procedures, i.e., enter the number of pages containing information.

7*b*. NUMBER OF REFERENCES: Enter the total number of references cited in the report.

8*a*. CONTRACT OR GRANT NUMBER: If appropriate, enter the applicable number of the contract or grant under which the report was written.

8*b*, 8*c*, & 8*d*. PROJECT NUMBER: Enter the appropriate military department identification, such as project number, subproject number, system numbers, task number, etc.

9*a*. ORIGINATOR'S REPORT NUMBER(S): Enter the official report number by which the document will be identified and controlled by the originating activity. This number must be unique to this report.

9*b*. OTHER REPORT NUMBER(S): If the report has been assigned any other report numbers *(either by the originator or by the sponsor)*, also enter this number(s).

10. AVAILABILITY/LIMITATION NOTICES: Enter any limitations on further dissemination of the report, other than those imposed by security classification, using standard statements such as:

(1) "Qualified requesters may obtain copies of this report from DDC."

(2) "Foreign announcement and dissemination of this report by DDC is not authorized."

(3) "U. S. Government agencies may obtain copies of this report directly from DDC. Other qualified DDC users shall request through
_______________."

(4) "U. S. military agencies may obtain copies of this report directly from DDC. Other qualified users shall request through
_______________."

(5) "All distribution of this report is controlled. Qualified DDC users shall request through
_______________."

If the report has been furnished to the Office of Technical Services, Department of Commerce, for sale to the public, indicate this fact and enter the price, if known.

11. SUPPLEMENTARY NOTES: Use for additional explanatory notes.

12. SPONSORING MILITARY ACTIVITY: Enter the name of the departmental project office or laboratory sponsoring *(paying for)* the research and development. Include address.

13. ABSTRACT: Enter an abstract giving a brief and factual summary of the document indicative of the report, even though it may also appear elsewhere in the body of the technical report. If additional space is required, a continuation sheet shall be attached.

It is highly desirable that the abstract of classified reports be unclassified. Each paragraph of the abstract shall end with an indication of the military security classification of the information in the paragraph, represented as *(TS)*, *(S)*, *(C)*, or *(U)*.

There is no limitation on the length of the abstract. However, the suggested length is from 150 to 225 words.

14. KEY WORDS: Key words are technically meaningful terms or short phrases that characterize a report and may be used as index entries for cataloging the report. Key words must be selected so that no security classification is required. Identifiers, such as equipment model designation, trade name, military project code name, geographic location, may be used as key words but will be followed by an indication of technical context. The assignment of links, rules, and weights is optional.